الجمهوريـــة الجزائريـــة الديمقراطيـــة الشعبـــة

People's Democratic Republic of Algeria

وزارة التعليـــــــم العالـــــــي والبـــحـــث العلمـــي

Ministry of Higher Education and Scientific Research

جامعـــــــة غردايـــــــة

University of Ghardaia

كليـــة العلـــوم والتـــكنـــولـــوجيـــا

Faculty of Science and Technology

قســم التعليـــم المشتـــرك في العلـــوم والتـــكنـــولـــوجيـــا

MEMORY

For obtaining the master's degree

Domain: Material Sciences

Sector: Physics

Specialty: Energy physics and renewable energies

Theme

Assessment of the combustion of biogas in a turbulent diffusion flame

Supported on: 15/06/2025

Presented by: ***- Zineb BENAHMED*** ***- Feriel LAOUAR***

In front of the jury composed of:

Dr. .... Hadj Yahia SEBAA	**Univ Ghardaia**	**President**
Dr. .... Laghouiter Oum Kelthoum	**Univ Ghardaia**	**Examiner**
Dr. .... Ouassila BENCHADI	**Univ Ghardaia**	**Examiner**
Pr. .....Djemoui LAlMI	**Univ Ghardaia**	**Supervisor**
Pr. .....Djilali GHOBRINI	**Univ Ghardaia**	**Co-supervisor**

Academic year: 2024/2025

Thanks and appreciation

بِسْمِ اللَّهِ الرَّحْمَنِ الرَّحِيمِ
{وَقُلِ ٱعْمَلُوا۟ فَسَيَرَى ٱللَّهُ عَمَلَكُمْ}

Praise be to God, who has bestowed His blessings upon us and enabled us to complete this research.
By His grace and generosity, knowledge increases and goals are achieved.

We extend our sincere thanks and appreciation to our supervisor (Dr. LALMI Djemoui.) for his sound guidance and constant assistance, which had a profound impact on the completion of this research.

We especially thank our families and friends, who provided us with psychological and moral support throughout the research period and helped us overcome difficulties.
We pray to God to guide everyone to what is best, and that this research will be a modest addition to the field of renewable energy.

Dedication

We dedicate this work with love and gratitude to everyone who has been by our side, believed in us, and supported us every step of this journey:

To our families:
Thank you for being our constant source of strength. Your love, patience, and encouragement have given us the motivation to continue, even in the most difficult moments. This achievement is the fruit of your support and trust in us.

To our esteemed professors:
We express our sincere gratitude for all the knowledge and guidance you have provided us throughout our academic journey.

To our dear supervisor dr.DJEMOUI LALMI:
We are deeply grateful for your continuous support, valuable advice, and trust in us. Your guidance has played a significant role in shaping and completing this work.

To our friends and colleagues:
For every kind word, every moment of encouragement, and every laugh that has eased our burdens on the road—thank you for being there, making the experience more beautiful and lighter.

Finally, to both of us, for all the hard work we've put in, for all the challenges we've faced and overcome together, for every moment of doubt when we believed in our abilities. This memo is not just a scientific study; it's a true reflection of the spirit of cooperation, determination, and maturity we've acquired.

May this achievement be the beginning of a journey filled with success, God willing.

Abstract

This study aims to conduct a comprehensive assessment of biogas combustion within the context of a turbulent diffusion flame, with the goal of deepening the scientific understanding of the physical and chemical mechanisms governing this type of combustion and improving its efficiency in energy applications.

The focus of the study is on the combustion of a binary mixture composed of methane and hydrogen, with an investigation into how different mixing ratios affect flame behavior, stability, and energy conversion efficiency.

The study includes a detailed analysis of the flame's dynamic and thermal properties, examining temperature distribution, flow patterns, and mixing characteristics between the fuel and oxidizer under strong turbulence conditions. The obtained results were compared to experimental data, showing a highly positive correlation.

The stability of the flame was also evaluated under the influence of different hydrogen ratios (30% and 40%), given hydrogen's crucial role in enhancing flame speed and increasing temperature. Environmental performance indicators were also considered by monitoring pollutant emissions from combustion, particularly nitrogen oxides (NOx), with the aim of proposing clean and environmentally friendly combustion solutions.

This study can serve as a foundation for advanced mathematical and numerical models to simulate the complex reactions occurring within turbulent flames, enabling a precise analysis of chemical reactions and flow fields.

Keywords : biogas , combustion , turbulent flamme , simulation , swirl and NO_X

Résumé

Cette étude vise à effectuer une évaluation complète du processus de combustion du biogaz dans le contexte d'une flamme de diffusion turbulente, dans le but d'approfondir la compréhension scientifique des mécanismes physiques et chimiques qui régissent ce type de combustion, et d'améliorer son efficacité dans les applications énergétiques.

L'accent a été mis sur la combustion d'un mélange binaire composé de méthane et d'hydrogène, avec l'étude de l'impact de différentes proportions de mélange sur le comportement de la flamme, sa stabilité et son efficacité de conversion énergétique.

L'étude comprend une analyse détaillée des propriétés dynamiques et thermiques de la flamme, en examinant la distribution de la température, le schéma d'écoulement, et les caractéristiques de mélange entre le carburant et l'oxydant dans des conditions de turbulence intense, en comparant les résultats obtenus avec des données expérimentales, avec une correspondance très positive. La stabilité de la flamme a également été évaluée sous l'effet de différentes proportions d'hydrogène (30 % et 40 %), en raison de son rôle essentiel dans l'amélioration de la vitesse de flamme et de l'élévation de la température, tout en prenant en compte les indicateurs de performance environnementale, à travers le suivi des émissions polluantes issues de la combustion, notamment les oxydes d'azote (NOx), dans l'objectif de proposer des solutions de combustion propres et respectueuses de l'environnement.

Cette étude peut servir de base à des modèles mathématiques et numériques avancés pour la simulation des réactions complexes à l'intérieur de la flamme turbulente, permettant une analyse précise des réactions chimiques et des champs d'écoulement.

Mots-clés : biogas , combustion , flamme turbulente , simulation , swirl et NO_X.

الملخص :

تهدف هذه الدراسة إلى إجراء تقييم شامل لعملية احتراق البيوغاز ضمن سياق لهب انتشاري مضطرب، وذلك بهدف تعميق الفهم العلمي للآليات الفيزيائية والكيميائية التي تحكم هذا النوع من الاحتراق، وتحسين كفاءته في التطبيقات الطاقوية. تم التركيز في هذه الدراسة على احتراق خليط ثنائي مكوَّن من الميثان والهيدروجين، مع دراسة تأثير نسب الخلط المختلفة على سلوك اللهب، واستقراره، وفعاليته في تحويل الطاقة.

شملت الدراسة تحليلًا مفصلًا للخصائص الديناميكية والحرارية للهب، حيث تم فحص توزيع درجات الحرارة، ونمط الجريان، وخصائص الاختلاط بين الوقود والمؤكسد في ظل ظروف اضطراب قوية من خلال مقارنة النتائج المحصلة بنتائج تجريبية، حيث كان التطابق جد إيجابي. كما تم تقييم مدى استقرار اللهب تحت تأثير نسب مختلفة من الهيدروجين 30%و40%، لما له من دور أساسي في تحسين سرعة اللهب وزيادة درجة الحرارة، مع الاخذ بعين الاعتبار مؤشرات الأداء البيئي، من خلال تتبع انبعاثات الملوثات الناتجة عن الاحتراق، ولا سيما أكاسيد النيتروجين(NOx) ، وذلك بهدف تقديم حلول احتراق نظيفة وصديقة للبيئة. يمكن الاعتماد على هذه الدراسة في نماذج رياضية وعددية متقدمة لمحاكاة التفاعلات المعقدة داخل اللهب المضطرب، قد يتيح إمكانية إجراء تحليل دقيق للتفاعلات الكيميائية ومجالات الجريان.

الكلمات المفتاحية: الغاز الحيوي، الاحتراق، اللهب المضطرب , المحاكات , الدوامة و أكسيد الازوت .

Summary

Chapter III : Materials and Methods

LIST OF FIGURES

LIST OF TABLES

NOMENCLATURE

Symbole	Intitulé	Unité
A	Surface area (rayonnante)	[m]
$\boldsymbol{Q_L}$	Lower Calorific Value (PCI)	[kJ/kg]
$\mathbf{Q_H}$	Higher Calorific Value (PCS)	[kJ/kg]
$\boldsymbol{w}$	Moisture content (wt% moisture in fuel / 100)	[---]
H	Hydrogen content (wt% hydrogen in fuel / 100)	[---]
ρ	The gas density	[kg/m³]
D	Molecular diffusivity	[m²/s]
$\mathbf{u_i}$	Velocity component (i-th direction)	[m/s]
$\dot{\omega}_\mathbf{c}$	The reaction rate of the reaction progress variable	[kg/m³·s]
$\mathbf{D_Z}$	Mixture fraction diffusivity	[m²/s]
$\boldsymbol{S_L}$	Laminar flame speed	[m/s]
$\boldsymbol{\delta_L}$	Laminar flame thickness	[m]
$\boldsymbol{\tau_f}$	Flame time scale	[s]
$\boldsymbol{T_F}$	Chemical or mixing time scale	[s]
$\mathbf{T_\eta}$	Kolmogorov time scale	[s]
Re	Reynolds number	[—]

Da	Damköhler number	[—]
$\boldsymbol{Da^{fl}}$	Local flame Damköhler number	[—]
Ka	Karlovitz number	[—]
$\widetilde{\boldsymbol{X}}$	Mean scalar dissipation rate	[1/s]
$\widetilde{\mathbf{X}}_{\mathbf{st}}$	Scalar dissipation rate at stoichiometric surface	[1/s]
$(\boldsymbol{Q} \mid \mathbf{z}_{\boldsymbol{st}})$	Conditional average of Q at z = z_{st}	Same as Q
U	Velocity	[m/s]
L	Characteristic length	[m]
μ	Dynamic viscosity	[Pa•s] or [kg/(m•s)]
$\mathbf{G_X}$	$Axial\ momentum\ flux$	[kg•m/s²] or [N]
R	$Air\ inlet\ radius$	$[m]$
D	Characteristic length (burner nozzle outlet diameter)	[m]
$\mathbf{G_\varphi}$	$Tangential\ momentum\ flux$	[kg•m/s²] or [N]

General Introduction:

In light of the growing global challenges associated with the intensive reliance on fossil fuels, and amid increasing environmental concerns related to greenhouse gas emissions and global warming, the search for sustainable and cleaner energy alternatives has become more urgent than ever[1]. Among these alternatives, biogas emerges as a promising renewable energy source, derived from the anaerobic digestion of organic matter and offering both environmental and economic benefits[2].

Biogas, primarily composed of methane (CH_4), carbon dioxide (CO_2), and hydrogen (H_2), is widely recognized for its potential as a clean energy carrier. However, its utilization in combustion systems presents specific challenges due to its variable composition and the complex behavior of turbulent flames. In particular, understanding the combustion dynamics of biogas mixture sespecially under turbulent diffusion conditions is essential for improving system performance and reducing pollutant emissions such as nitrogen oxides (NO_x)[3].

This study aims to numerically investigate the combustion of biogas within a turbulent diffusion flame using advanced Computational Fluid Dynamics (CFD) techniques. A binary mixture of methane and hydrogen is selected to represent biogas, and different mixing ratios are explored to evaluate their influence on flame stability, temperature distribution, flow dynamics, and environmental impact. The work adopts a multidisciplinary approach that combines concepts from thermodynamics, fluid mechanics, combustion chemistry, and numerical modeling.

The importance of this research lies in its contribution to the development of accurate and predictive CFD models that support the design of efficient and environmentally friendly combustion systems[4].

It offers valuable insights into the physical and chemical mechanisms governing biogas combustion and serves the broader goal of supporting the transition to sustainable energy technologies.

The study is organized into three chapters:

-Chapter I presents a bibliographic study that introduces biogas, its sources, properties, and historical development.

-Chapter II explores the theoretical aspects of combustion and turbulence, including flame classifications, reaction mechanisms, and turbulence modeling techniques such as DNS, LES, and RANS.

-Chapter III details the simulation methodology, including the computational setup, boundary conditions, and analysis of the numerical results regarding flame behavior and pollutant formation at different hydrogen ratios.

The outcomes of this research demonstrate that increasing hydrogen content enhances flame characteristics and combustion efficiency, while also highlighting the need to manage associated environmental impacts. These findings represent a step forward in the development of cleaner combustion strategies and contribute meaningfully to the advancement of sustainable energy research.

Chaptre I

Bibliographic study

Chapter I: Bibliographic study

Introduction:

Since the mid-20th century, the world has witnessed a massive population growth, with the number of people increasing from 2.5 billion in 1950 to 6.2 billion in 2002. It is expected to reach between 8 and 9 billion by 2050. Despite the relative slowdown in this population growth, it continues to place significant pressure on global energy resources. With the historical reliance on fossil fuels since the Industrial Revolution in the 19th century, there is an urgent need to seek alternative energy sources that are renewable, cleaner, and have less negative impact on the environment[5].

Currently, only about 20% of global energy needs are met by renewable sources such as solar, wind, and biomass.

In developed countries, the share of renewable energy sources like solar, wind, nuclear, biomass, and geothermal energy is steadily increasing in the energy mix. However, in developing countries, the primary reliance remains on fossil fuels and biomass.

Biomass is a major source of bioenergy in rural areas of developing countries due to its abundance, scalability, and cost-effectiveness compared to other renewable energy sources. It also contributes to effective waste management by converting plant and animal waste into clean energy. Various types of biomass fuels produce biogas, including wood, charcoal, agricultural residues, household waste, animal waste, and energy crops. Biogas production is considered one of the most environmentally friendly technologies for bioenergy, as it enhances the stability of gaseous fuel supplies. Since the energy crisis in the 1970s, biogas has become one of the leading alternatives to fossil fuels as a source of renewable natural gas[6].

Biogas is a product of the anaerobic fermentation of organic materials. The composition of biogas varies depending on the type of organic material used and the operating conditions, but it primarily consists of methane (CH_4), carbon dioxide (CO_2), nitrogen (N_2), oxygen (O_2), hydrogen sulfide (H_2S), and hydrogen (H_2). Due to its methane content, biogas can be used as a fuel to generate heat and electricity.

Biogas is considered a natural product and a promising alternative to fossil fuels, especially given the negative impacts of fossil fuels, such as exacerbating global warming and reliance on geopolitical factors. One of the most common and straightforward methods of utilizing biogas is

direct combustion, owing to its low cost and minimal maintenance requirements. This type of use does not require the removal of hydrogen sulfide or moisture from the biogas, and its conversion efficiency to heat in dual-fuel burners reaches approximately 80-90%. However, raw biogas cannot be directly used in commercial burners designed for natural gas or liquefied petroleum gas (such as propane and butane). This is because the air-to-fuel ratio in biogas is insufficient for stable combustion due to its high carbon dioxide content. Therefore, using biogas requires the installation of new burners equipped with separate systems. Additionally, since biogas contains corrosive components (such as water and hydrogen sulfide), condensation of these components must be prevented by maintaining the furnace temperature above the dew point. This means the furnace must first be heated using natural gas or liquefied petroleum gas to ensure the required operating temperature is achieved[7].

I .1. General information on biogas:

I. 1.1. Biogas:

Biogas is a gas produced from the decomposition of organic animal or plant materials in an oxygen-free environment, a process known as methanization. This phenomenon can occur naturally in swamps or spontaneously in landfills containing organic waste. It can also be artificially induced in bio digesters to treat wastewater sludge, industrial, or agricultural waste[8].

Biogas is considered a renewable energy source derived from biomass, typically composed of approximately 65% methane (CH_4) and 35% inert carbon dioxide (CO_2). It is characterized by its chemical composition and physical properties, making it a promising fuel. The term "biogas" encompasses a variety of gases produced from the treatment of diverse organic waste whether industrial, animal, or household in origin.

Each cubic meter of biogas contains about 6 kWh of thermal energy. When converted into electricity using specialized generators, it produces approximately 2 kWh of useful electricity, while the remaining energy is transformed into heat, which can be utilized for heating purposes[5].

I. 1.2. Chemical composition of biogas:

The composition of biogas varies depending on the production source. The presence of H_2S, CO_2, and water increases its corrosiveness, necessitating the use of appropriate materials. The gas composition in a fermenter is influenced by the type of substrate,its organic matter content, and the feeding rate of the methanizer [9].

Tab I.1: Chemical composition of biogas [9]

Components	Household waste	WWTP sludge	Agricultural waste	Waste from the agri food industry
CH_4 % vol	50-60	60-75	60-75	68
CO_2 % vol	38-34	33-19	33-19	26
N_2 % vol	5-0	1-0	1-0	-
O_2 % vol	1-0	< 0,5	< 0,5	-
H_2O % vol	6 (à 40 ° C)	6 (à 40 ° C)	6 (à 40 ° C)	6 (à 40 ° C)
Total % vol	100	100	100	100
H_2S mg/m^3	100 - 900	1000 – 4000	3000 – 10 000	400
NH_3 mg/m^3	-	-	50 - 100	-
Aromatics mg/m^3	0 - 200	-	-	-
Organochlorines or organofluorines mg/m^3	100-800	-	-	

I.3. Physical Characteristics:

Due to its composition, biogas exhibits distinctive properties when compared to natural gas and propane. It is significantly lighter than air and generates half the amount of energy per unit volume during combustion compared to natural gas[9].

Tab I.2: physical characteristics of biogas [9].

Types of gas	Biogas 1 Household waste	Biogas 2 agri-food industry	Natural gas
Composition	60% CH_4 33% CO_2 1% N_2 0% O_2 6% H_2O	68% CH_4 26% CO_2 1% N_2 0% O_2 5 % H_2O	97,0% CH_4 2,2% C_2 0,3% C_3 0,1% C_{4+} 0,4% N_2
PCS kWh/m^3	6,6	7,5	11,3
PCI kWh/m^3	6,0	6,8	10,3
Density	0,93	0,85	0,57
Masse volumique (kg/m^3)	1,21	1,11	0,73

I.4. Importance of using biogas:

Biogas has gained significant attention because it is readily available wherever life exists, and it is easy to produce and use. One crucial fact to note is that methane has a global warming potential 21 times higher than CO_2. When biogas is burned, methane is converted into CO_2, reducing its greenhouse gas impact by 20 times.

Extracting methane from waste and using it for heat or electricity generation prevents waste from decomposing in open environments, thereby reducing methane emissions into the atmosphere. Additionally, the energy provided by biogas replaces fossil fuels, which are major contributors to climate change.

Biogas is considered carbon-neutral because the carbon released during its combustion originates from the carbon absorbed by plants in the natural cycle[5].

I.5. Sources of Biogas Production:

Organic materials of plant or animal origin that have not yet undergone full decomposition or fermentation are used as a primary source for biogas production. These materials are known as biomass and include various types of waste that can be classified into five main categories:

- Agricultural waste and residues from related industries.
- Municipal solid waste.
- Urban wastewater.
- Animal waste.
- Industrial solid and liquid waste, including industrial sludge.

Chapter I: Bibliographic study

Biogas is a colorless, flammable gas produced through the biological degradation of organic matter in the absence of oxygen. It originates from "biogenic materials" and is generated via anaerobic digestion of degradable substances such as biomass, animal manure, green waste, and agricultural residues like cassava and sugarcane.

Biogas consists of a mix of gases, mainly methane (CH_4) and carbon dioxide (CO_2), along with 1–5% of other gases like hydrogen (H_2). Bacteria play a key role in producing this gas under anaerobic conditions. Thanks to its energy content, biogas serves as an effective fuel source for heating and cooking. It can also be utilized in anaerobic digesters to generate electricity and heat using gas engine.

The production of biogas began in the second half of the 19th century. It results from the anaerobic digestion of various organic materials such as human and animal waste, kitchen and agricultural residues, municipal waste, and algal or plant biomass, all within a balanced carbon cycle. Biogas is considered a renewable energy source, similar to solar, wind, and geothermal energy[10].

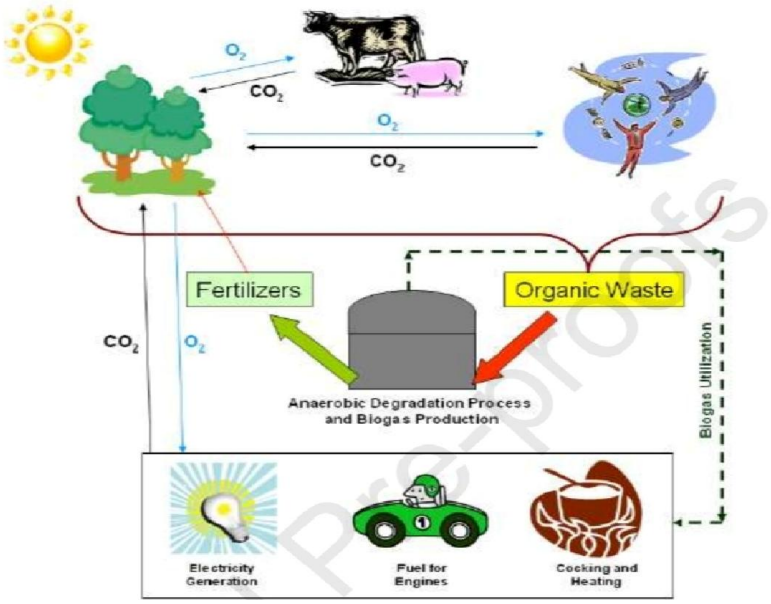

Figure I.1: Biogas cycle in nature [10]

I.2. Evolution of biogas use:

Historical records suggest biogas was first utilized around 3000 BCE in ancient Assyria, where it served to warm bathing waters. Centuries later, in the 1600s, Flemish scientist Jan Baptist van Helmont observed that decomposing organic materials released combustible vapors. He also introduced the term "gas" derived from the Greek "chaos" into scientific terminology[11].

In a remarkable 1764 correspondence, Benjamin Franklin described to Joseph Priestly how he witnessed combustible vapors igniting above a shallow New Jersey marsh - one of history's earliest documented encounters with natural biogas phenomena.

The scientific understanding of these marsh gases took shape in 1776 when Italian researcher Alessandro Volta chemically identified methane as their primary component. This discovery gained further significance after John Dalton's 1804 work on methane's molecular structure, paving the way for European experimentation with practical biogas applications. Russian researchers made substantial contributions to this emerging field. During 1875 experiments, scientist Popov observed that riverbed organic matter initiated biogas production at temperatures as low as 6°C. When heated to 50°C, gas output increased dramatically while maintaining consistent composition: 65% combustible methane, 30% carbon dioxide, 1% hydrogen sulfide, plus minimal nitrogen, oxygen and carbon monoxide. Later, microbiologist V.L. Omeliansky would decode the complex bacterial processes driving anaerobic decomposition.

European innovators began harnessing this knowledge by 1881, demonstrating biogas's potential for both heating and illumination. The English city of Exeter became a pioneer in 1895, powering an entire neighborhood's street lighting system with gas derived from sewage containment tanks. Similar systems soon emerged in Bombay, where collected biogas was adapted to fuel combustion engines[12].

The early 1900s saw German engineers Imhoff and Blank (1914-1921) develop patented digestion chambers with integrated heating elements to optimize output. World War I's fuel shortages accelerated biogas adoption across Europe, with equipped agricultural operations maintaining functionality despite technological limitations. A crucial 1930s advancement came from researcher Boswell, who significantly improved production efficiency by combining manure with other

organic materials. Britain emerged as an implementation leader when Birmingham's 1911 treatment facility became the first large-scale operation to simultaneously process wastewater and generate electricity. By the 1920s, British engineers had developed multiple refined digester models. This innovation spread to Algeria in 1938 with Issman and duselier's 10-cubic-meter facility designed specifically for solid organic waste.

The energy crises of World War II revived interest in alternative fuels. France and Germany constructed approximately 2,000 manure-based biogas plants by the mid-1940s, while Soviet forces noted Hungary's widespread adoption of sealed manure digestion systems. However, postwar fossil fuel abundance temporarily diminished biogas's appeal until the 1970s oil crisis sparked renewed global interest - particularly in Asia, where tropical climates and high population density favored low-maintenance systems [12].

Currently, biogas use varies significantly among the world's leading adopters, with distinct patterns emerging in power generation, grid injection, and transportation:

Electricity and heat production: Germany is the world leader in biogas-fired electricity and heat generation, followed by Brazil, Canada, France, and Finland. These countries primarily use biogas in combined heat and power (CHP) plants to maximize energy efficiency.

Grid injection: Denmark and Switzerland dominate the development of biogas into biomethane for direct injection into natural gas grids, with purification processes ensuring compatibility with existing infrastructure.

Transport Fuel: Sweden and Finland have pioneered the use of refined biomethane as a sustainable vehicle fuel, primarily in:

- Compressed biogas (bio-CNG) for urban transport fleets

- Liquefied biogas (bio-LNG) for heavy transport

Industrial Applications: France, Norway, and Brazil widely use biogas in industrial processes, capitalizing on its potential to replace fossil fuels in manufacturing and processing[13] .

Conclusion:

At the conclusion of this chapter, which covered the theoretical and fundamental aspects of biogas, it is clear that this renewable energy source represents a promising solution to overcome the environmental and energy challenges facing the contemporary world, especially in light of the continuous rise in energy demand and the increasing environmental pressures associated with the intensive use of fossil fuels. We discussed in detail the nature of this gas, in terms of its origin, its chemical and physical components, and its properties that make it suitable for use in various fields, such as electricity generation, heating, and biofuel for transportation.

The most important conclusion reached through this presentation is that biogas is not only a clean and environmentally friendly alternative to traditional sources, but also represents an opportunity to recycle various types of organic waste, whether agricultural, household, or industrial, within the framework of a circular economy system that seeks to reduce waste and achieve sustainability. On the other hand, a study of the evolution of biogas use over the ages to the present day has shown that global interest in this energy is growing, and that countries that have invested in developing this technology have been able to create more flexible and independent energy systems, especially during times of crisis.

Understanding the basic properties of biogas, its history, and its sources of production is a fundamental and essential step that allows us to build a solid foundation for moving to experimental studies aimed at evaluating the combustion of this gas in a turbulent diffusion flame and analyzing its performance in terms of efficiency and gas emissions. This theoretical background also allows us to place the scientific approach in its proper framework and link it to the global energy and environmental context, ultimately serving the goal of this research: contributing to the development of clean and efficient energy solutions in light of the transition to renewable energy.

Chapter I: Bibliographic study

Reference:

[1]. Intergovernmental Panel on Climate Change. (2021). Climate change 2021: The physical science basis. Cambridge University Press

[2]. Yadvika, Sreekrishnan, T. R., Kohli, S., & Rana, V. (2004). Enhancement of biogas production from solid substrates using different techniques: A review. Bioresource Technology, 95(1), 1–10.

[3]. Li, T., Cai, J., & Han, X. (2012). Combustion characteristics of biogas and biogas–hydrogen mixtures. International Journal of Hydrogen Energy, 37(11), 8804–8814.

[4]. Versteeg, H. K., & Malalasekera, W. (2007). An introduction to computational fluid dynamics: The finite volume method (2nd ed.). Pearson Education.

[5]. Aggab, Y., & Zaouia, Y. (2016). *Simulation numérique de la combustion du biogaz hydrogéné en régime sans flammes* [Master's thesis, Université Larbi Ben M'hidi Oum-El-Bouaghi].

[6]. Idika, C., & Aimikhe, V. J. (n.d.). Non-linear regression models for predicting biogas yields from selected bio-wastes

[7]. Leonov, E. S., & Trubaev, P. A. (2021). Analysis of biogas content influence on the flame properties. *IOP Conference Series: Materials Science and Engineering, 1089*(1), 012032.

[8]. Deublein, D., & Steinhauser, A. (2008). Biogas from Waste and Renewable Resources: An Introduction. Wiley-VCH.

[9]. Naskéo Environnement. (2009). Composition du biogaz. Biogaz Énergie Renouvelable.

[10]. Jameel, M. K., Mustafa, M. A., Ahmed, H. S., Mohammed, A. J., Ghazy, H., Shakir, M. N., Lawas, A. M., Mohammed, S. K., Idan, A. H., Mahmoud, Z. H., Sayadi, H., & Kianfar, E. (2024). Biogas: Production, properties, applications, economic and challenges: A review. Results in Chemistry, 7, 100911.

[11]. National Grid. (2023, February 23). What is biogas?

[12]. Fluid. (n.d.). Biogas technologies and applications. Fluid Biogas.

[13]. IEA Bioenergy Task 37. (2024). State of the biogas industry in 12 member countries of IEA Bioenergy Task 37. International Energy Agency..

Chaptre II

Combustion and Turbulence

Chapter II: *Combustion and Turbulence*

Introduction:

Combustion is a fundamental physical and chemical phenomenon that has contributed to human development throughout the ages. It has been a pillar of technological progress, both in energy generation and in many industrial applications. However, accurately understanding and controlling this phenomenon remains a scientific challenge, given the complexity of the accompanying chemical reactions and their interaction with physical phenomena such as heat transfer and gas kinetics.

Among the most common and complex forms of combustion is turbulent combustion, which is characterized by a continuous interaction between the random flow of gases and chemical reactions. This type of combustion is the most widespread in practical applications due to its ability to enhance the mixing of components and improve combustion efficiency. However, it poses significant challenges in predicting and analyzing its behavior.

When observing the development of a flame or smoke from a combustion process in a calm environment, three main regions can be distinguished: a base region where the flow is uniform or laminar, followed by a transition region where turbulence begins to appear in the form of eddies, and then an upper region where turbulent flow predominates, where tracking particle motion becomes extremely complex.

To address the complexity of turbulent combustion, different numerical modeling approaches have been developed, mainly Direct Numerical Simulation (DNS), Large Eddy Simulation (LES), and Reynolds-Averaged Navier-Stokes (RANS). DNS resolves all scales of turbulence and chemical interactions without simplification, offering high accuracy but requiring enormous computational resources. LES provides a compromise by resolving large turbulent structures while modeling smaller scales, making it suitable for many industrial cases. RANS, the most widely used model in engineering applications, relies on time-averaged equations and turbulence models, offering faster results with lower computational cost.

Chapter II: *Combustion and Turbulence*

The importance of studying turbulent combustion lies in its combination of two major challenges: understanding the aerodynamics of turbulent flows and understanding multiple, simultaneous chemical reactions. This interplay between physics and chemistry makes the study of turbulent flames a rich field of interest to researchers, especially in light of the move towards the use of alternative fuels such as biogas, which requires accurate combustion models to ensure efficient and sustainable performance [1-2]

Chapter II: *Combustion and Turbulence*

II.1. The combustion

II.1.1. Definition of combustion :

Combustion is an exothermic chemical process in which a fuel, whether solid, liquid or gaseous, reacts with an oxidizer (oxygen, air, etc.), releasing heat energy. During this reaction, new substances known as exhaust gases are formed, which arise mainly from the combination of fuel and oxygen. For example, when a fuel containing hydrogen and carbon such as gasoline is burned, the combustion products include water (resulting from the combination of hydrogen with oxygen) and carbon dioxide (resulting from the combination of carbon with oxygen). In addition, if combustion occurs in air (which contains a percentage of nitrogen), other compounds such as nitrogen oxides (NO_x) may appear as a result of the reaction of nitrogen with oxygen [3].

- The combustion reaction can be represented by the following chemical equation:

$$C_xH_y + \left(x + \frac{y}{4}\right) O_2 \rightarrow xCO_2 + \frac{y}{2} H_2O + \text{Energy} \quad \text{.....(II.1)}$$

II.1.2. Fire Triangle :

The fire triangle is a simple model used to understand the basic elements needed for a fire to occur. Each side of the triangle represents one of the three ingredients needed for a fire to exist: oxygen, fuel, and heat. Fire is a chemical reaction, and if any of these ingredients are absent, a fire cannot occur or continue [4].

Figure II.1: Fire triangle [4]

II.1.3 Combustion classifications:

II.1.3.1. Combustion Based on Fuel Efficiency :

Incomplete combustion occurs when fuel burns in a limited supply of oxygen or air, resulting in the formation of carbon monoxide, soot, water vapor, and heat. This type of combustion happens when there is a blockage in the gas burner, restricting the air supply, causing liquefied petroleum gas (LPG) to burn with a yellow-orange flame and release soot.

complete combustion occurs when fuel burns in the presence of sufficient air, producing carbon dioxide, water vapor, and heat. When LPG burns in an adequate air supply, it produces a blue flame, indicating complete combustion.

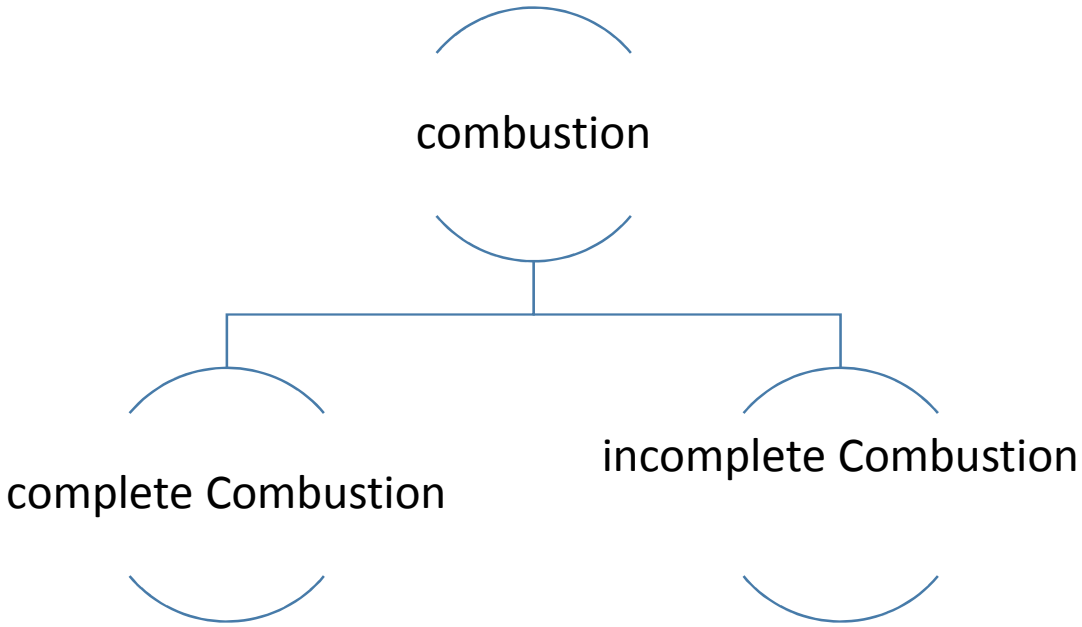

Figure II.2: Fuel-Efficient Combustion.

II.1.3.2. Combustion Based on Reaction Nature and Speed:

Rapid combustion: This occurs when a substance ignites instantly and produces heat and light in a very short time. An example of this is lighting a gas stove in the kitchen.

Spontaneous combustion: This occurs when a substance ignites without the need for an external heat source, catching fire suddenly on its own. Examples include forest fires or the spontaneous burning of phosphorus at room temperature.

Explosion: This is a type of combustion where a sudden reaction occurs, accompanied by the release of heat, light, and sound. An example is the explosion of firecrackers when exposed to heat and pressure.

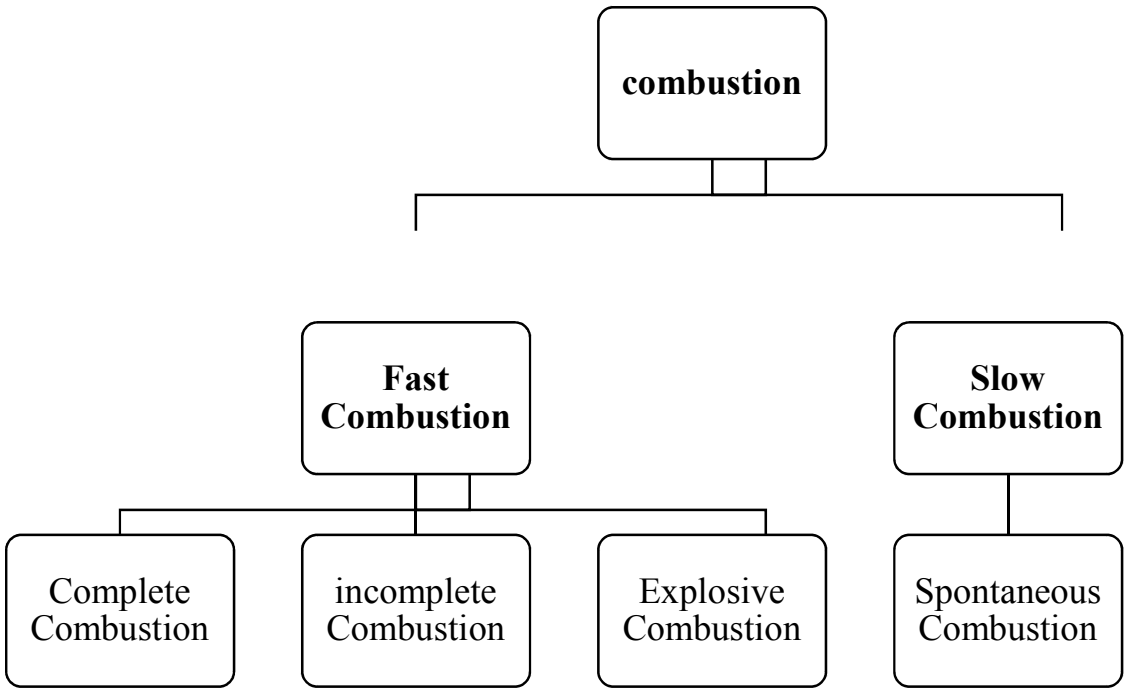

Figure II.3: Combustion Categorized by Reaction Mechanism and Speed.

II.1.4. Calorific value and energy released:

The calorific value (CV) of a fuel is the amount of heat released during its complete combustion, representing the energy content per unit mass or volume. It is a critical property of fuel, as higher calorific values result in greater energy yield and improved engine performance. The calorific value is typically expressed in units such as kilojoules per kilogram (kJ/kg) or joules per liter (J/L) and depends on the fuel's chemical composition[5].

The two types of calorific values for fuel are[6]:

Higher or Gross calorific value (HCV): When a fuel containing hydrogen burns in the presence of oxygen, water vapor is produced as one of the combustion products. If this vapor is condensed into water at room temperature, it releases additional thermal energy known as latent heat of condensation. This energy, when added to the energy released from combustion, forms what is called the Higher Calorific Value (HCV), which represents the total energy released per unit mass of fuel.

Lower or Net Calorific Value (LCV) : If the water vapor produced during combustion is not condensed into liquid water, the net energy obtained from the complete combustion of a unit quantity of fuel is referred to as the Lower Calorific Value (LCV) or Net Calorific Value. For practical purposes, LCV is commonly used in calculations.

In brief, the Lower Calorific Value (LCV) is the amount of heat released without accounting for the heat of condensation of water vapor, while the Higher Calorific Value (HCV) includes it. The calorific value of a fuel is measured using a bomb calorimeter.

- The relationship between the Higher Calorific Value (HCV) and the Lower Calorific Value (LCV) of a fuel can be expressed by the following equation[7]:

$$Q_L = Q_H - 2454(w + 9H) \quad \text{.....(II.2)}$$

WHERE: Q_L: Lower Calorific Value (kJ/kg).

Q_H: Higher Calorific Value (kJ/kg).

w: wt% moisture in fuel/100.

H: wt% hydrogen in fuel/100.

Table II.1: HCV and LCV of fuels [2].

Fuel type	**HCV (KJ/kg)**	**LCV (KJ/kg)**
Coal (anthracite)	30000–33000	28000–31000
Natural gas	50000–55000	45000–50000
Diesel	45000–46000	42000–43000
Benzene	44000–47000	41000–44000
Biofuel	18000–22000	16000–20000

II.1.5. Laminar combustion modes:

The combustion mode can be defined as the state of the mixture before it reaches the flame zone in the injection system. As is known, there are two main types of flames: non-premixed flames (also known as diffusion flames) and premixed flames[8].

-Laminar combustion can occur in three modes:

1. Premixed combustion.
2. Non-premixed combustion.
3. Partially premixed combustion.

II.1.5.1. Laminar Premixed Flames:

A premixed flame is a type of combustion that occurs when a prepared mixture of fuel and oxidizer (such as air) is burned in specific ratios. Once the mixture ignites, the process sustains itself due to the heat energy released. Most of the chemical reactions occur in a thin region that separates the burned gases from the unburned ones. The flame propagates through the mixture until all the fuel and oxidizer are completely consumed[9].

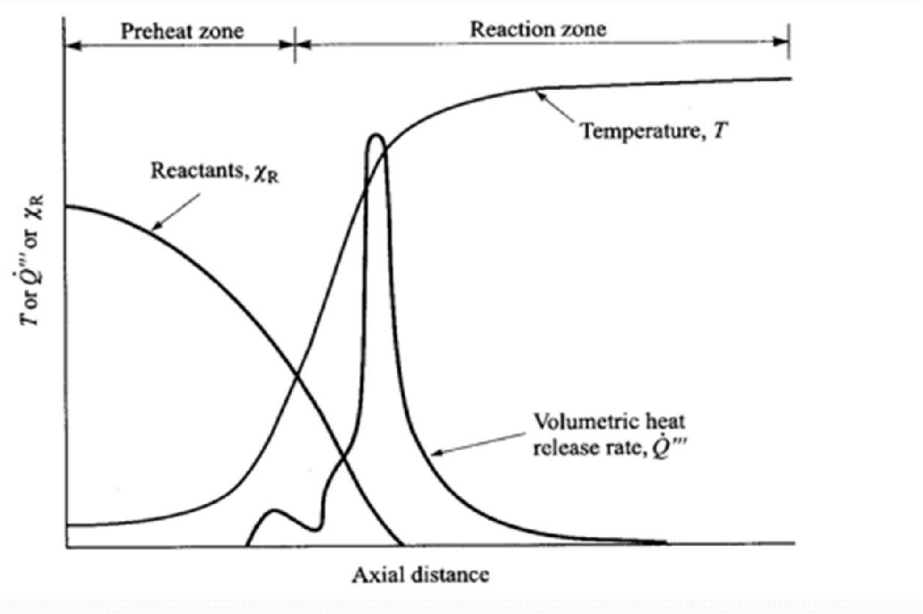

Figure II.4: Temperature and Reaction Rate Distribution in a Premixed Flame [9].

- **Reaction progress variable:**

The extent of completion of the chemical reaction can be determined using a variable known as the Reaction Progress Variable, denoted by c. This variable starts at 0.0 in the unburned gases and gradually increases until it reaches 1.0 in the fully burned products. In this analysis, the reaction progress variable c is defined based on the fuel mass fraction Y_F (i.e., the mass fraction of methane CH_4) [10].

-The reaction progress variable transport is governed by:

$$\frac{\partial \rho c}{\partial t} + \frac{\partial \rho u_i c}{\partial x_i} = \frac{\partial}{\partial x_i}\left(\rho D \frac{\partial c}{\partial x_i}\right) + \dot{\omega}_c \qquad \text{.....(II.3)}$$

Where: -$\boldsymbol{\rho}$ is the gas density.

-$\boldsymbol{D}$ is the mass diffusivity of the species based on which the reaction progress variable is defined.

- $\boldsymbol{u_i}$ is the velocity component.

-$\boldsymbol{\dot{\omega}_c}$ is the reaction rate of the reaction progress variable.

II.1.5.2. Laminar diffusion flame:

It is a type of combustion that occurs when the fuel and oxidizer are separated before the reaction, unlike a premixed flame where they are mixed before combustion. In this type of flame, the combustion process is controlled by the rate of diffusion and mixing of the components, not just by the speed of the chemical reaction[11].

-The following figure shows the structure of a diffusion flame:

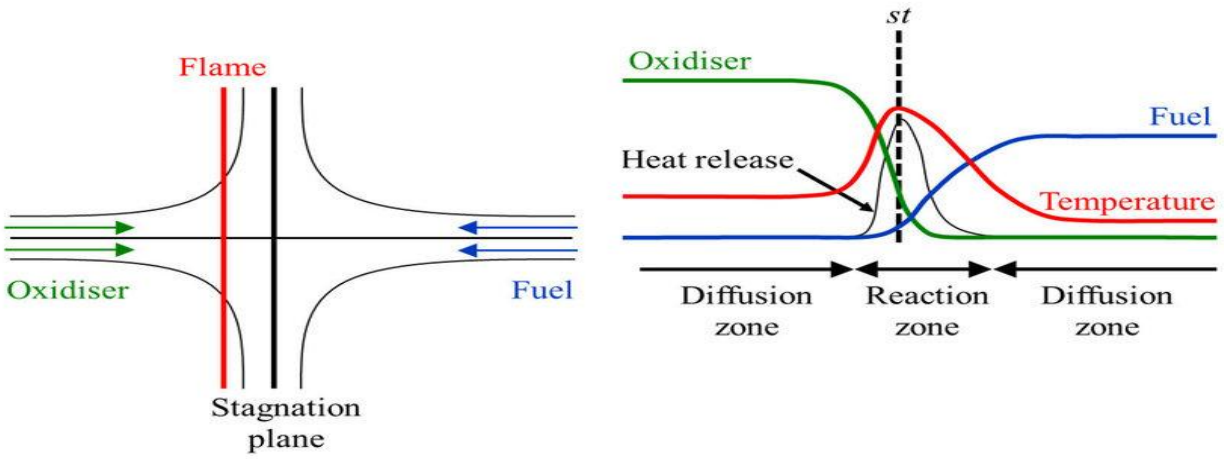

Figure II.5: Theoretical representation of diffusion flame structure [11].

- **Mixture fraction Z:**

Mixture fraction is a dimensionless quantity used in combustion studies to describe the concentration of the mixture between fuel and oxidizer. It is defined as the ratio of the mass of fuel to the total mass of the mixture (fuel + oxidizer). Its value is 1 in the case of pure fuel and 0 in the case of pure oxidizer, Its transport equation is written[12]:

$$\frac{\partial \rho Z}{\partial t} + \frac{\partial \rho u_i Z}{\partial x_i} = \frac{\partial}{\partial x_i}\left(\rho D_Z \frac{\partial Z}{\partial x_i}\right) \quad \text{(II.4)}$$

where: D_Z is the mixture fraction diffusivity with the boundary conditions.

II.1.6. Combustion regimes for turbulent flames:

The Damkohler number (Da) is a fundamental factor in analyzing turbulent combustion, as it helps evaluate flame stability in scramjet engines by integrating the effects of fuel-air mixing, chemical reaction rates, and flow residence time in the combustor.

The Damkohler number is defined as the ratio of flow residence time to the sum of mixing and chemical reaction times, expressed as:

$$\boldsymbol{Da} = \frac{\tau}{\tau_c} = \frac{\text{Integral time scale of turbulence}}{\text{Chemical time scale}} \quad \text{..... (II. 5)}$$

To achieve flame stabilization, Da must be ≥ 1, which requires reducing mixing and chemical reaction times while increasing flow residence time in the combustor. At high hypersonic speeds (M > 8), this can be achieved more easily by accelerating chemical reactions and prolonging flow duration. However, at lower speeds (5 < M < 8), flame stabilization becomes more challenging due to lower stagnation temperature and pressure, which slow down chemical reactions and reduce autoignition potential.

II.1.6.1.Regimes in Premixed Turbulent Combustion:

Turbulent premixed combustion occurs when chemical reactions interact with fluid turbulence, resulting in a wide range of spatial and temporal scales. These interactions play a crucial role in determining flame propagation speed, stability, and efficiency, particularly in applications such as gas turbines and internal combustion engines[13].

To understand the mechanisms of premixed turbulent combustion and the structure of the turbulent flame, the temporal and spatial scales of an unperturbed laminar flame considered a planar, one dimensional flame propagating at a constant speed with a constant thickness are compared with the corresponding scales of turbulence. The laminar flame is characterized by its speed S_L , thickness δ_L, and time scale:

$$\tau_S = \frac{S_L}{\delta_L} \quad \text{(II. 6)}$$

So we have:

$$Da = \frac{1}{\delta}\frac{S_L}{\grave{u}} \quad \text{(II. 7)}$$

-A new dimensionless number appears, known as the **Karlovitz number**, which is defined as the ratio of the chemical time scale T_F to the Kolmogorov time scaleT_η It is named after Béla Karlovitz and is expressed by the following relation:

$$Ka = \frac{T_F}{T_\eta} = \left(\frac{\grave{u}}{S_L}\right)^{3/2}\left(\frac{L}{\delta_L}\right)^{-1/2} = \frac{Re_T^{1/2}}{Da} \quad \text{(II. 8)}$$

From this, we conclude:

$$Re = Da^2 Ka^2 \quad \text{(II. 9)}$$

-By analyzing these dimensionless numbers and the orders of magnitude of the phenomena, several distinct combustion regimes can be identified. The Borghi diagram is commonly used to represent these different regimes:

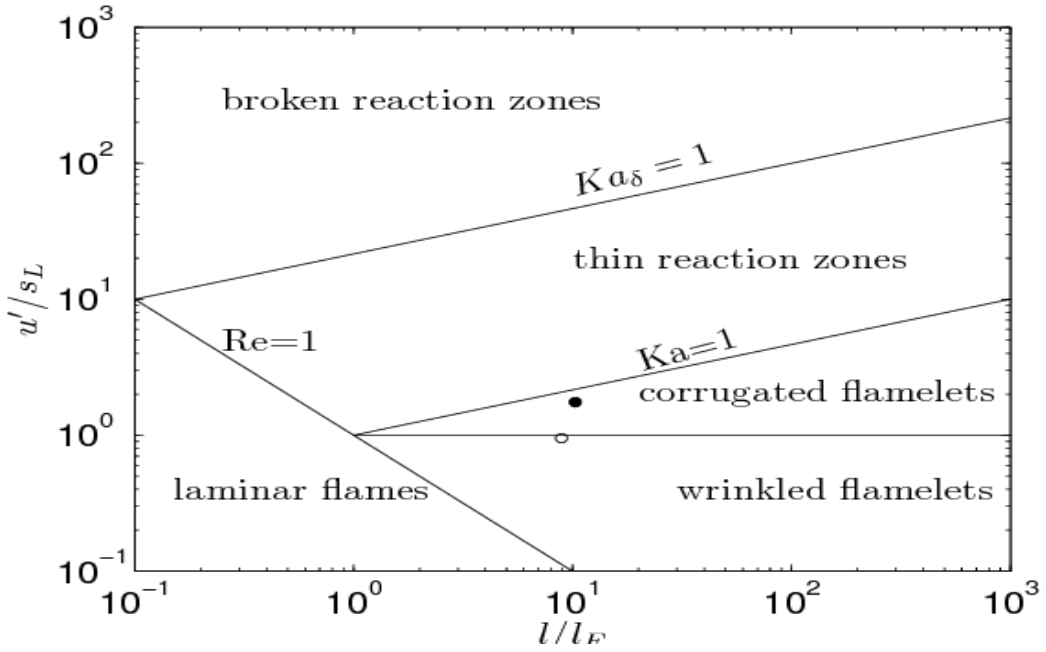

Figure II.6: Borghi diagram[14].

II.1.6.2. Diffusion flame turbulence:

Classifying combustion regimes in diffusion flames is more challenging due to the absence of a fundamental flame speed, with its thickness **δ** being primarily influenced by aerodynamic effects.

To classify distinct combustion regimes, turbulence timescales serve as a useful analytical tool.

-Borghi outlines several scenarios:

- When chemical reactions occur much faster than turbulence effects (τc < τη), the Damköhler number is high, and the flame retains a laminar-like structure. This corresponds to the folded flamelet regime.
- Conversely, when chemical kinetics are slower relative to turbulence scales (τc > τη), local flame extinction may occur due to excessive stretching forces, defining the flamelet regime with local extinctions.
- For high Reynolds numbers (Re > Re_critique), small-scale turbulence interactions significantly alter the internal structure of the flamelets to the point where they no longer maintain their typical characteristics.

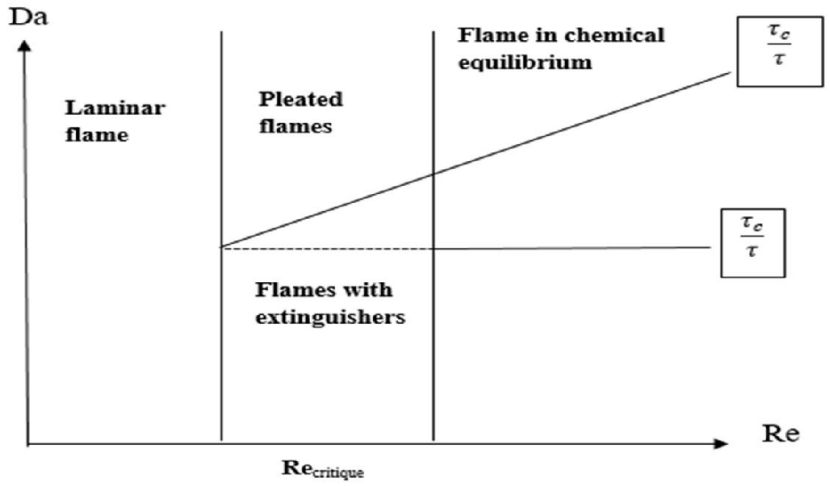

Figure II.7: Diagram for turbulent diffusion flames[15]**.**

- Cue not and Poinsot present a more detailed diagram derived from DNS simulations that examine the interaction between a diffusion flame and a pair of vortices.

The conditional average of $\boldsymbol{Q}$ at the stoichiometric surface z = $\mathbf{z}_{st}$ is represented by $(\boldsymbol{Q} \mid \mathbf{z}_{st})$. The mean scalar dissipation rate $\tilde{\chi}$st is typically unknown. However, assuming that turbulence governs the flame structure, the local diffusion layer can be treated as a steady, constant-density diffusion layer, establishing a direct link between $\widetilde{\boldsymbol{X}}$ and $\widetilde{\boldsymbol{X}}_{\boldsymbol{st}}$ (Poinsot and Veynante, 2012). From this, the local flame Damköhler number is defined as[16]:

$$\boldsymbol{Da^{fl}} = \frac{\boldsymbol{\tau_f}}{\boldsymbol{\tau_c}} \approx \left(\widetilde{\boldsymbol{X}}_{\boldsymbol{st}}\boldsymbol{\tau_c}\right)^{-\mathbf{1}} \quad \text{(II. 10)}$$

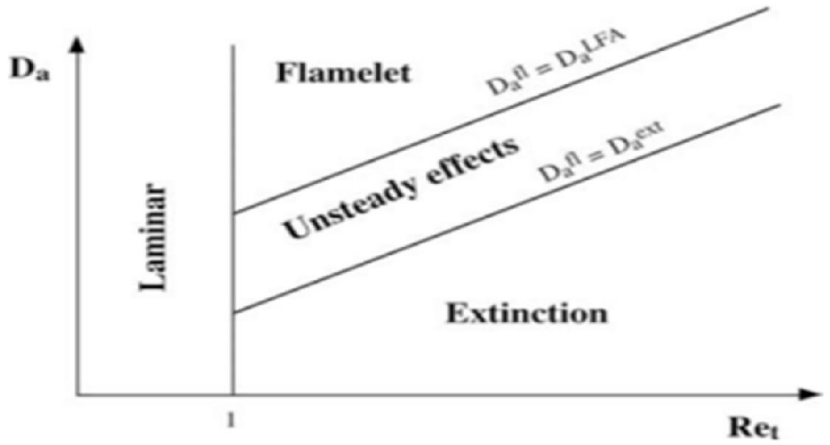

Figure II.8: Turbulent diffusion flame combustion diagram in (Da, Re_t) space [17]

Chapter II: *Combustion and Turbulence*

II.2. Turbulent Flow in combustion

II.2.1. Reynolds' Experiment (1883):

Reynolds demonstrated turbulence in a simple manner through an experiment illustrated in Figure (II.9) [1].

In 1883, Osborne Reynolds conducted a groundbreaking experiment to demonstrate the transition to turbulent flow. He investigated the behavior of water flow at different flow rates by introducing a thin jet of dyed water into the center of the flow inside a larger pipe.

The larger pipe was made of glass, allowing direct observation of the dyed water's motion. A flow-control valve at the pipe's end enabled adjustments to the water velocity. At low velocities, the dyed stream remained distinct along the entire length of the pipe. However, as the velocity increased, the dyed layer eventually broke up and dispersed across the fluid's cross-section. This marked the transition from laminar to turbulent flow. Reynolds determined that this transition was governed by a dimensionless parameter, later known as the Reynolds number[2].

He found that the transition typically occurred within a Reynolds number range of 2000 to 13,000, depending on the smoothness of the inlet conditions. Under carefully controlled conditions, the transition could be delayed up to a Reynolds number of 40,000. Conversely, when the entrance was rough, the transition culd occur at Reynolds numbers as low as 2000[18].

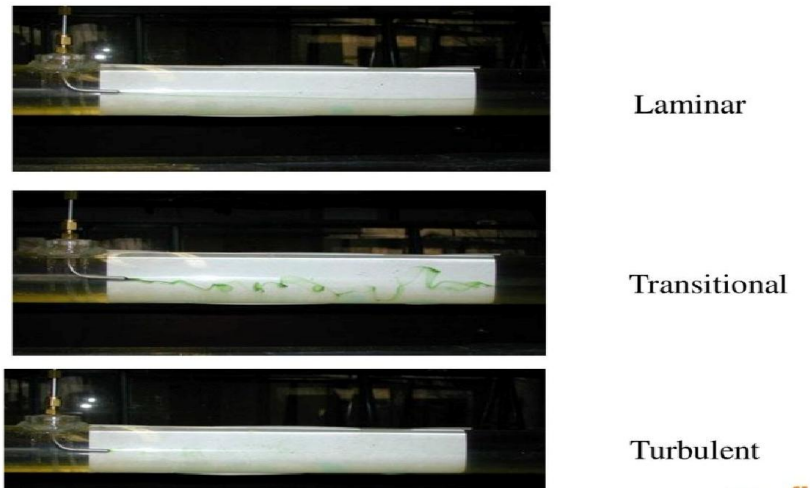

Figure II.9: Reynolds Experience 1883[19].

II.2.2. The laminar-turbulent transition:

The onset of turbulence is caused by various factors, primarily the increase in the Reynolds number, which compares the nonlinear convection terms to the viscous dissipation term:

$$\mathbf{Re} = \frac{U.\rho.L}{\mu} \quad \text{.....(II.11)}$$

As the Reynolds number increases, the flow topology changes, indicating the transition from a laminar to a turbulent regime. The specific Reynolds number value varies depending on the type of flow.

However, external forces such as Archimedean forces and the Coriolis force can also influence the onset of turbulence. It is important to note that the transition mechanisms from a laminar to a turbulent regime are complex and three-dimensional[20].

II.2.3. Kolmogorov Cascade:

Unlike the study of coherent structures in turbulent flows, a theory has significantly contributed to understanding turbulence: Kolmogorov's theory (1941). This theory is based on a statistical approach to turbulence and assumes that vortices within the flow exist within a specific size range, limited by two main scales:

- The largest scale of the flow, which is determined by the geometry of the flow. Examples include the diameter of a cylinder, the diameter of a chimney, or the height of a car.
- The smallest scale of the flow, which depends on the viscosity of the fluid. This scale is known as the Kolmogorov scale or the viscous dissipation scale.

The approximate relationship between these two scales is given by the following equation:

$$\frac{L}{\eta} = \mathrm{Re}^{\frac{3}{4}} \quad \text{.....(II.12)}$$

Where Re is the Reynolds number[1].

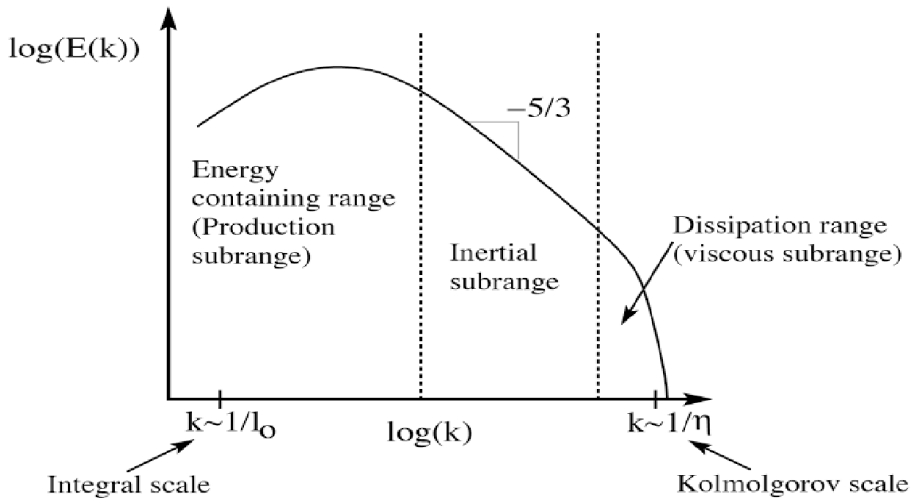

Figure II.10: Kinetic energy flux in a turbulent flow [21].

The energy "cascade" theory suggests that vortices acquire energy from larger scales and progressively transfer it to smaller scales, continuing this process down to the smallest scale in the flow, denoted as. Energy is produced when large flow structures form, such as during flow separation, while energy dissipation occurs when vortices vanish entirely downstream of an obstacle. When the rate of energy production matches that of energy dissipation, the turbulence is considered to be in a state of "equilibrium" [1].

II.2.4. The Main Turbulence Models:

There are three main methods for modeling turbulent flow[22]:

- Direct numerical simulation, in which the aim is to represent all physical phenomena (DNS).
- Large-eddy simulation, in which only the largest eddies are represented as a function of time (LES).
- Averaged simulation, in which only the average flow is represented (RANS).

II.2.4.1 The direct numerical simulation (DNS):

The direct simulation of instantaneous Navier-Stokes equations is currently limited to flows with low Reynolds numbers and simple or even overly simplified geometric configurations compared to industrial applications. This approach is mainly used as a research tool to conduct numerical experiments in academic contexts.

The Kolmogorov viscous dissipation scale provides an estimate of the critical size beyond which vortices are rapidly dissipated due to molecular viscosity, preventing their further development. Consequently, direct turbulence simulation is only viable when the discretization grid is on the same order of magnitude as this scale. Given that the ratio between large vortices and the Kolmogorov scale is approximately $Re^{\frac{3}{4}}$, the number of computational nodes must, in theory, be proportional to $Re^{\frac{9}{4}}$ in each spatial direction.

-If we consider the expression for the **Kolmogorov** scale:

$$l_\eta = l \cdot Re_l^{-\frac{3}{4}} \quad \text{.....(II.13)}$$

where **l** represents the scale of energy-carrying vortices, which is approximately equal to the size of the studied installation, and $Re_l = u' \frac{l}{\vartheta}$ is the **Reynolds number** at scale **l**, it can be observed that the computational grid size decreases significantly as **Re** increases.

When the **Reynolds number** is high, the gap between the largest and smallest scales in the flow becomes so significant that it is impossible to account for all these scales in a single calculation.

Under these conditions, the most precise simulations require computational grids of approximately 1024^3 points and are performed on machines equipped with hundreds of parallel processors. Such calculations are highly complex to implement and generate massive amounts of data, making their management and analysis challenging. For this reason, these simulations are primarily reserved for academic and research purposes. They are typically applied in cases where the **Reynolds number** is below **1000**, serving as numerical experiments often used to validate turbulence models, which will be discussed later [23].

II.2.4.2. Large Eddy Simulation (LES):

Since direct numerical simulation (DNS) of all turbulent flow scales is constrained by computational power, Large Eddy Simulation (LES) has been developed as a more approximate and less computationally expensive alternative. In LES, the flow equations are solved numerically, but only the large-scale eddies are explicitly computed, while the smaller scales are not resolved. As a result, the simulation provides an approximation of the actual flow, with the smallest turbulent structures missing. To compensate for this limitation, additional modeling is applied to account for the effects of small-scale eddies and energy dissipation.

The fundamental concept of LES is based on the idea that small-scale turbulence has a weaker influence compared to larger eddies, which contain most of the turbulent energy and stresses and interact more significantly with the mean flow. Additionally, small-scale turbulence tends to be more isotropic, making it more suitable for separate modeling. However, despite these simplifications, the computational requirements for LES remain substantial, especially when applied to complex real-world flow scenarios[24].

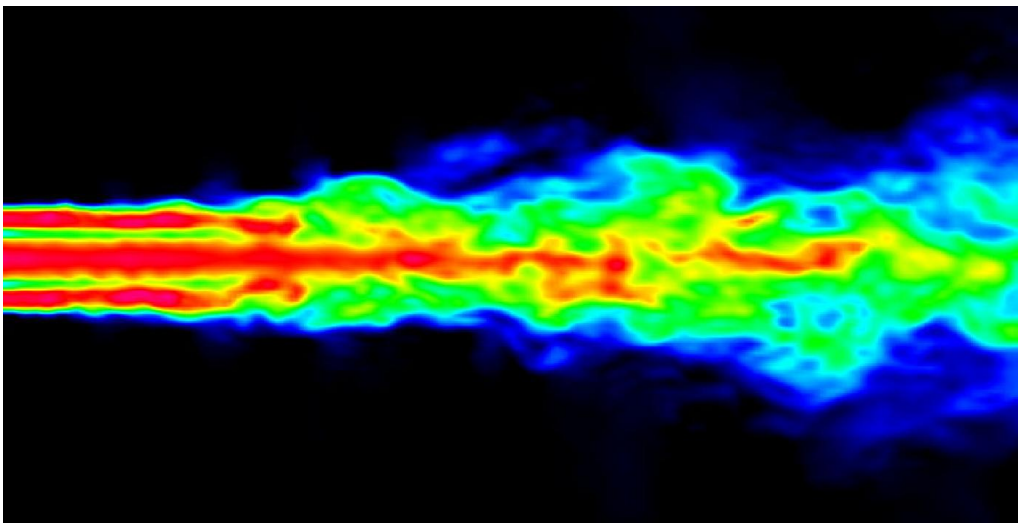

Figure II.11: Simulation of a gas jet by the SGS method [25].

II.2.4.3. Simulation of the averaged Navier-Stokes equations:

This approach focuses on simulating only the mean flow over time, where all fluctuations are filtered out and modeled through the effect of turbulent viscosity.

There are two main types of averaging methods:

- **Ensemble averaging**: The experiment is repeated **N** times under identical experimental conditions, ensuring the same flow behavior in each trial. The resulting data is then averaged.
- **Time averaging**: A single experiment is conducted over a long period, and the mean is calculated from the collected data over this duration.

If the averaging time is sufficiently long, time averages are, in principle, independent of time. However, if the averaging time is short—meaning it is less than the characteristic time of the studied phenomenon—time averages remain dependent on time. Similarly, ensemble averages can also be time-dependent, such as in flows with dominant periodic frequencies.

When time and ensemble averages do not coincide, the system is considered **inhomogeneous**. This occurs, for example, when a system evolves over time or when initial conditions significantly influence the flow behavior.

On the other hand, when time and ensemble averages are independent of time and equal, the process is said to be **"statistically stationary**[20].

The following figure defines a rough graphical comparison of the main simulations:

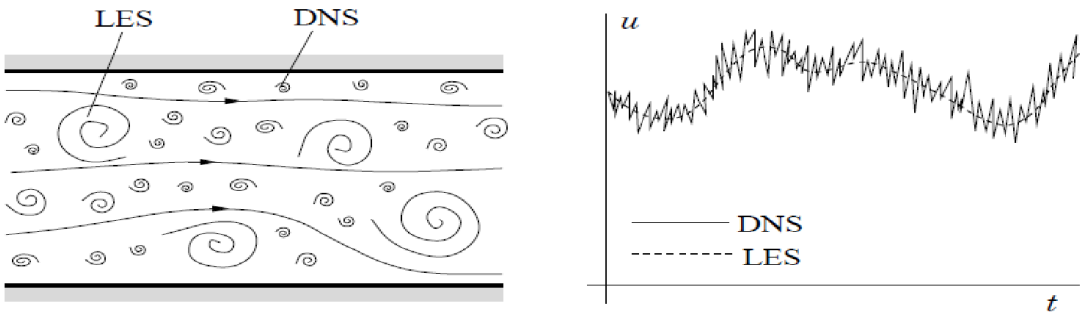

Figure II.12 : graphical comparison of the different simulations[26].

II.2.5. Characteristics of Turbulent Flow:

- Turbulent flow is inherently three-dimensional
- It is unsteady, meaning it does not include steady flows. However, some steady flows can exhibit complex properties, such as Lagrangian chaos.
- It is characterized by uncertainty, both in measurement and in calculations.
- It has a random, disordered, and fluctuating nature, with a spatial redistribution of its quantities.
- It enhances mixing and diffusion of transported quantities, such as the interaction between milk and coffee, the propagation of temperature in a fluid, or the dispersion of cigarette smoke.
- This type of flow covers a wide range of dynamically active scales, resulting in a kinetic energy spectral density (defined by frequency or wavenumber) that is continuous and nonzero over several orders of magnitude.

- Turbulent flow is chaotic in the sense that even a small perturbation can grow over time. This makes a strictly deterministic description impractical. As a result, instantaneous velocity fields at different times in the same flow can be significantly different, even if the initial conditions were nearly identical. This characteristic implies that the study of turbulent flows should be approached using statistical methods.

- Noise: Turbulent flows generate noise due to acoustic sources resulting from pressure fluctuations within the fluid.
- The effects of turbulence are sometimes positive and sometimes negative:

- **Positive effects**: Increased mixing improves combustion, for example, and enhances aircraft lift.
- **Negative effects**: Dispersion of pollution.

- The velocity vector at a point varies randomly in both direction and magnitude[20].

II.2.6. The Simulation of the averaged Navier-Stokes (R.A.N.S) equations:

The formulation of transport equations for averaged quantities is based on applying Reynolds decomposition to the instantaneous equations, followed by the averaging operation. This process leads to the derivation of the so-called moment equations, also known as the Reynolds-Averaged Navier-Stokes (RANS) equations[1].

II.2.6.1. Conservation of mass equation:

$$\frac{\partial \overline{\rho}}{\partial t} + \frac{\partial}{\partial x_i}\left(\overline{\rho} \widetilde{u_i}\right) = 0 \quad \text{.....(II.14)}$$

II.2.6.2. Momentum conservation equation:

$$\frac{\partial \overline{\rho} \widetilde{u_i}}{\partial t} + \frac{\partial}{\partial x_i}\left(\overline{\rho} \widetilde{u_i} \widetilde{u_j}\right) + \frac{\partial \overline{P}}{\partial x_i} = \frac{\partial}{\partial x_i}\left(\overline{\tau_{ij}} - \overline{\rho} \widetilde{u_i'' u_j''}\right) \quad \text{.....(II.15)}$$

II.2.6.3. Energy conservation equation:

$$\frac{\partial}{\partial t}(\rho \bar{h}) + \frac{\partial}{\partial x_i}(\overline{\rho u_i h}) = \frac{\partial}{\partial x_i}(\lambda \frac{\partial \bar{T}}{\partial x_i} - \rho \overline{u_i' h'}) + \dot{Q} \quad \text{.....(II.16)}$$

II.3. The swirl effect*:*

II.3.1. The number of swirls≪ S ≫ :

To characterize the initial flow, two main quantities are generally used:

The first is the Reynolds number (Re), well known in fluid mechanics, which evaluates the ratio between inertial forces and viscous forces. The second quantity describes the initial intensity of the flow rotation and represents the ratio between the axial fluxes of tangential and axial momentum.

In this context, the flow is mainly characterized by a vortex, within which two distinct regions can be identified. The first is located near the axis of rotation, where the viscosity of the fluid plays a dominant role, causing the fluid to behave like a solid body rotating around the axis. The second

region, on the other hand, corresponds to an area where the fluid exhibits a more ideal behavior, being driven by the rotating fluid mass near the axis[2].

This type of flow is characterized by a dimensionless number:

$$Re = \frac{\rho.U.D}{\mu} \quad \text{.....(II.17)}$$

G_X = represents the axial momentum flux .

R = represents the air inlet radius (m).

D = represents the characteristic length (diameter of the burner nozzle outlet).

U = represents the axial velocity $\left(\frac{\text{m}}{\text{s}}\right)$.

G_φ : represnts the tangential momentum flux .

With:

$$s = \frac{G_\varphi}{RG_X} \quad Or \quad G_\varphi = \int_0^R 2\pi\rho r^2\, uw\, rd \quad \text{.....(II.18)}$$

$$G_X = \int_0^R 2\pi\rho r U^2 dr$$

This number allows for the comparison of the tangential momentum flux with that in the propagation direction. Thus, it provides an indication of the intensity of the swirling motion: the higher its value, the stronger the turbulence in the flow [2].

II.3.2. Swirling Flows:

A flow is described as "swirling" when the fluid exhibits rotational motion around its main flow direction. This type of flow is commonly encountered in various industrial applications.

For non-reactive flows, examples include cyclone separators, vortices formed in the wake of aircraft, and agricultural spraying equipment.

Regarding reactive flows, swirling motion is present in gas turbines, internal combustion engines, and certain industrial furnaces. Additionally, natural phenomena such as tornadoes and cyclones also fall into the category of swirling flows.

The main characteristic of these flows is the rotation of the fluid around itself, which creates a low-pressure region along its axis. This pressure drop can lead to the formation of a recirculation zone along the flow axis[2].

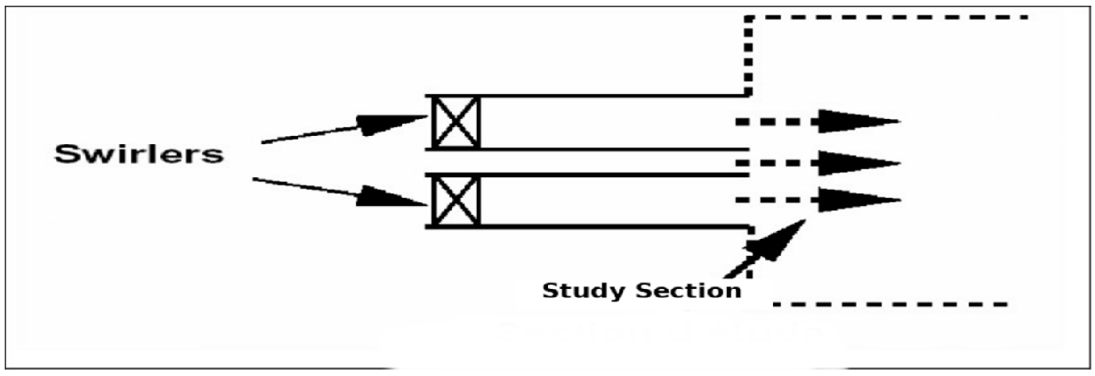

Figure II.13*:* Generic abrupt expansion used for applied studies of swirling flows[27].

II.3.3. Effect of Swirl on a Non-Reactive Flow:

Swirling flows can be categorized into two main types: low-swirl flows (S<0.6) and high-swirl flows (S>0.6).

- ***Low-Swirl Flows:***

In flows with a low swirl number, no recirculation zones are observed. The presence of swirl increases the entrainment of the surrounding stationary fluid and reduces the axial velocity of the flow. At lower swirl numbers, the velocity profile maintains a Gaussian shape up to approximately S<0.5. As the swirl number increases, both the jet-opening angle and the entrained mass flow gradually increase.

- ***High-Swirl Flows:***

When the swirl number exceeds approximately S=0.6, the longitudinal pressure gradients become insufficient to counteract the kinetic energy of the fluid particles. As a result, a toroidal recirculation zone forms within the flow. This recirculation region can be associated with a transition from supercritical to subcritical flow, similar to phenomena observed in shock waves or hydraulic jumps.

One of the defining characteristics of this recirculation zone is that its center shifts closer to the nozzle (or main injector), and its size increases as the swirl number rises[28].

II.3.4. Effect of Swirl on Reactive Flow:

Swirl is a commonly used technique in combustion due to its role in enhancing flame stability. When the swirl intensity reaches a certain level, a recirculation zone is formed, where unburned and burned gases mix, improving flow uniformity.

This zone acts as a reservoir for heat and reactive species near the burner exit, contributing to sustained combustion. Additionally, swirl enhances the entrainment process, leading to a reduction in flame size. This technique also allows for higher fuel velocities in diffusion flames and helps reduce the combustion chamber size in premixed combustion systems[28].

Conclusion

This chapter provides the conceptual and methodological framework essential for any rigorous scientific analysis of combustion phenomena in gaseous media, particularly in the context of turbulent flows and renewable energy applications. Multiple approaches were adopted to describe the complex physical and chemical processes involved in combustion, by linking dynamic and thermal parameters with reaction nature, flow regime, and the characteristics of the reactive medium. The diversity of flame types and the variability of their behavior under different operating conditions necessitate the use of dimensionless models, such as Damköhler and Karlovitz numbers, which enable the classification of combustion and thermal systems and help determine stability domains and transitional regions within reactive flows.

Moreover, numerical modeling stands as a cornerstone analytical tool in the study of turbulent flow, owing to its capacity to simulate interactions within complex environments that are often inaccessible through traditional experimental methods. Models such as DNS, LES, and RANS offer various levels of accuracy and representation, depending on computational resources and the intended analytical purpose, making model selection a methodological process intrinsically linked to the studied phenomenon.

In addition, the analysis of swirling flows represents a key step in understanding the mechanisms of flame stabilization and dispersion within combustion systems. Their direct impact on energy redistribution and the formation of recirculation zones plays a critical role in controlling flame propagation and reaction speed. Understanding turbulence effects on heat and mass transfer also allows for the identification of optimal operating conditions for high-efficiency combustion systems.

The interdisciplinary nature of this chapter—encompassing thermodynamics, fluid mechanics, and numerical modeling—reflects the necessary convergence of scientific domains for a comprehensive understanding of the complex phenomena associated with gaseous fuel combustion. This theoretical foundation constitutes a pivotal step for framing the upcoming practical work, whether it involves

numerical simulations or energy and environmental performance assessments of combustion systems based on alternative fuels such as biogas.

Reference :

[1]. Lalmi, D. (2018). Influence du Co et Contre Swirl d'écoulements sur les caractéristiques d'une flamme turbulente de diffusion [Doctoral dissertation, Université L'Arbi Ben M'Hidi d'Oum El Bouaghi]. Université OEB.

[2]. Atfi, L. Z., & Mouley, M. S. (2019). Contribution à l'étude d'une flamme produite dans un brûleur muni de swirl [Master's thesis, Université Ibn Khaldoun de Tiaret]. Département de Génie Mécanique, Faculté des Sciences Appliquées.

[3]. NASA Glenn Research Center. (n.d.). Combustion basics.

[4]. NW Fire Science Consortium. (n.d.). Fire facts: Fire triangle and fire behavior triangle.

[5]. Renewable and Sustainable Energy Reviews. (2017). Calorific value. Engineering.

[6]. Gujarati, P. (2020, January 7). What are the meaning of a higher calorific value (HCV) and a lower calorific value (LCV) of a fuel? Mechanical Duniya.

[7]. International Flame Research Foundation (IFRF). (2001, November 5). What is the relationship between the higher and lower calorific value of a fuel? IFRF Handbook.

[8]. International Journal of Hydrogen Energy. (2023). Combustion mode.

[9]. Lewis, B., & von Elbe, G. (2012). Combustion, flames and explosions of gases. Academic Press.

[10]. Awad, H. S. A. M., Abo-Amsha, K., Ahmed, U., & Chakraborty, N. (2021). Comparison of the reactive scalar gradient evolution between homogeneous MILD combustion and premixed turbulent flames.

[11]. Progress in Energy and Combustion Science. (2001). Diffusion flame.

[12]. Perry, B. A., Mueller, M. E., & Masri, A. R. (2017). A two mixture fraction flamelet model for large eddy simulation of turbulent flames with inhomogeneous inlets. Proceedings of the Combustion Institute, 36(2), 1767–1775.

[13]. Energy and Combustion Science. (1979). Premixed turbulent flame. Engineering.

[14]. Borghi, R., & Destriau, M. (1995). La combustion et les flammes. Éditions Technip.

[15]. Borghi, R., & Champion, M. (2000). Modélisation et théorie des flammes. Éditions Technip.

[16]. de Luca, G. (2021). Development of a dynamic LES model for turbulent diffusion flames [Doctoral dissertation, Université Paris-Saclay]. HAL Archives.

[17]. Danjaji, M. B., Hassan, M. I., & Nor, M. J. M. (2022). Regime diagram for non-premixed flames. In Experimental and numerical studies on the effects of oxidizer preheating in non-premixed flame characteristics. ResearchGate.

[18]. Fung, Y. C. (1990). Biomechanics: Motion, flow, stress, and growth (p. 569). Springer-Verlag.

[19]. SlidePlayer. (n.d.). Présentation en ligne.

[20]. Merrouchi, F. (2019). Simulation numérique des écoulements turbulents dans une conduite cylindrique [Master's thesis, Université de Batna 2].

[21]. Stoll, R. (2014). LES of turbulent flows: Lecture 3 (ME EN 7960-003). Department of Mechanical Engineering, University of Utah.

[22]. Benmansour, A. (2021). Simulation à grande échelle d'un écoulement autour d'un obstacle [Master's thesis, Université de Tlemcen].

[23]. Bouguerra, N. (2004). Simulation numérique de la structure d'un écoulement turbulent à l'échelle urbaine en configuration stratifiée ou non : cas d'un obstacle [Master's thesis, Université de Tunis El Manar].

[24]. Doran, P. M. (2013). Bioprocess engineering principles (2nd ed.). Academic Press.

[25]. CFTurbo. (n.d.). Recherche et développement.

[26]. Altadill, M. (2021). Études numériques (Oran de stabilité) de l'écoulement autour d'un cylindre. ITLR Report.

[27]. Bouras, F. (2006). Simulation de la combustion turbulente non-prémélangée par le modèle « L.E.S ». ResearchGate.

[28]. Bessanane, N. (2008). Simulation numérique de la combustion turbulente dans des géométries complexes [Master's thesis, Université de Batna 2].

Chapter III

Material and Methods

III. Materials and Methods

III.1. Experimental Configuration:

The selected configuration has been investigated experimentally using Laser Doppler Anemometry (LDA) It consists of two co-swirling airflows: one through a central nozzle (diameter 15 mm) and the other through an annular nozzle (inner diameter 17 mm, expanding to an outer diameter of 30 mm at the outlet). Methane (CH□) is injected as a non-swirling gaseous fuel via an annular slit between both air streams, resulting in significant premixing before ignition occurs a few millimeters upstream of the burner outlet.

The combustion chamber has a diameter $\boldsymbol{D_{CC}} = 4D_0$ and its length $\boldsymbol{D_{CL}} = 18D_0$

A 70% diameter reduction orifice is placed at the outlet to prevent backflow, which could otherwise occur due to pressure drops along the axis. This design accelerates the flow, transitioning it from subcritical conditions after vortex breakdown to supercritical conditions at the outlet [Escudier and Keller 1985]. This reduces the recirculation region's sensitivity to boundary conditions.

Air and methane flow rates were set to:$M_a = 64\ Kg/h$ and $M_f = 1.8\ kg/h$

Corresponding to an air equivalence ratio $\lambda = 2$ and a flow residence time of 180 ms $Y_{f.0} = 0.02735562$. the air stream was preheated to 400°C ($\rho = 1.0924\ kg/m^3$, $\mu = 1.95710^{-5}\ kg/s.m$) and distributed between the inner circular passage ($0.37M_a = 23.68\ Kg/h$, $35.80\ m/s$, $Re_i = 49962$)and the outer annular canal [1].

The global Reynolds number was estimated based on the average axial air velocity at the nozzle exit (z = 0) and the throat diameter, yielding a value based on:

$$U_0 = 34.83\ m/s$$

The swirl numberS_0 at the nozzle outlet is defined as the ratio of angular to axial momentum flux:

$$S_0 = \frac{\int_0^{R_0} \rho(\bar{U}\bar{W}r+\overline{u'w'}r)r\,dr}{R_0 \int_0^{R_0} \rho\left(\overline{u^2}+\overline{u'^2}\right)r\,dr} \quad \text{.....(III.1)}$$

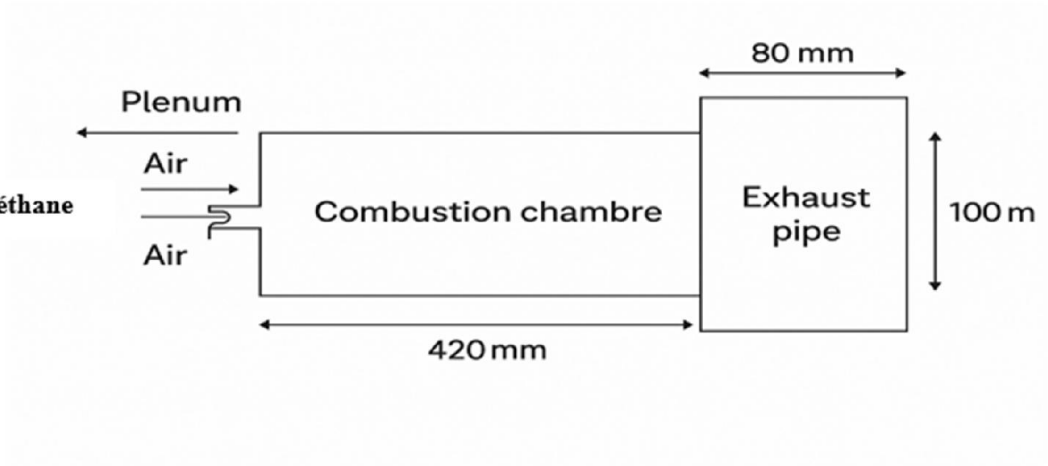

Figure III.1: Sketch of the geometrical configuration [2]

Geometrical swirl numbers S_{th} are estimated as $S_{th.in} = 0{,}46$ and of the outer air flow $S_{th.out} = 1.0$ total $S_{total} = 0{,}81$, as shown in Figure (III.1).

III.2. Meshing:

The first step is to develop a computational mesh that ensures the convergence of the numerical procedure and is capable of capturing all the variations of the different parameters within the computational domain. Table (1) and Figure (2) respectively present the mesh used in our simulation and its properties.

Table III.1: Mesh characteristics.

Settings	Values
Minimum volume (m^3)	1.249954e-10
Maximum volume (m^3)	2.715527e-08
Total volume (m^3)	3.352826e-03
Cells	hexahedral 837120
Nodes	853441
Between	Actual imposed speed
Exit	Pressure imposed
Walls	Adiabatic walls

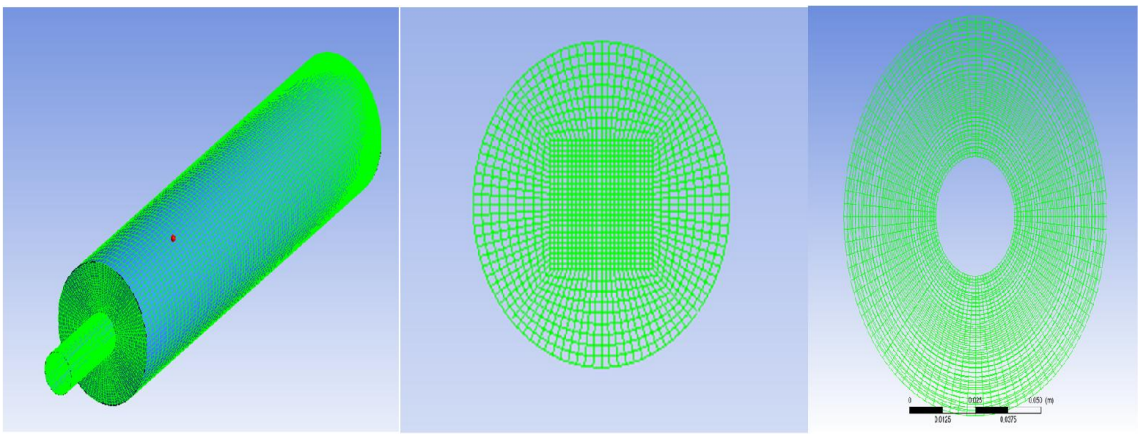

Figure III.2: Computational mesh of the combustion chamber domain

III.3. Boundary Conditions:

The boundary conditions are mostly given by the profile:

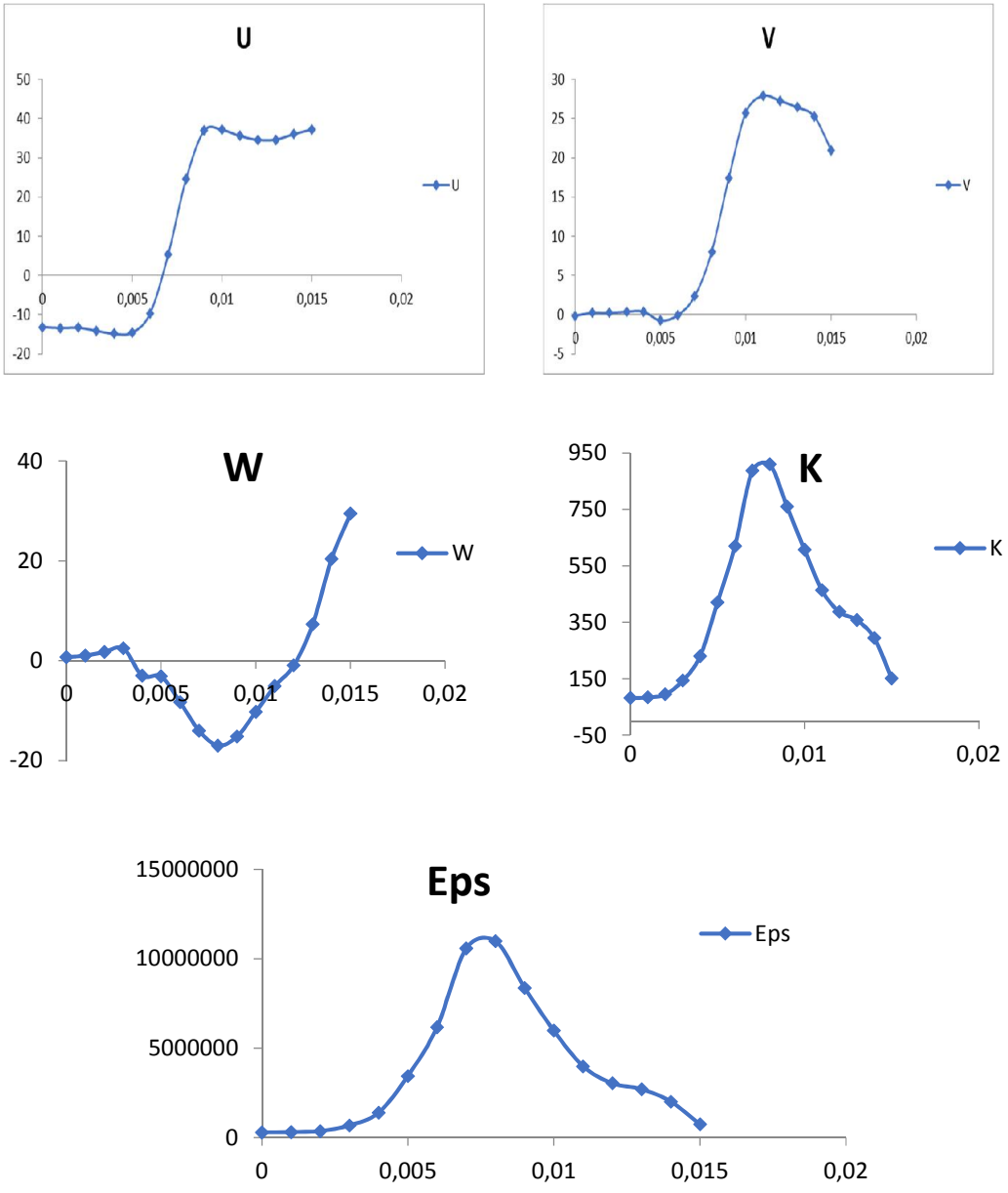

Figure III.3: Velocity profiles for boundary conditions at the inlet [3].

III.4. Velocity Profiles and Kinetic Energy in Cold Flow Conditions before Combustion:

Before combustion begins, the axial, radial, and tangential velocity profiles represent the airflow inside the chamber under cold flow conditions, where combustion effects are not yet present. These profiles reflect the influence of nozzle design and swirling motion on the velocity distribution. The tangential velocity indicates the degree of rotation in the flow, directly affecting the mixing of air and fuel, while the kinetic energy represents the amount of mechanical energy in the airflow, helping to understand its impact on the efficiency and characteristics of the combustion process later on.

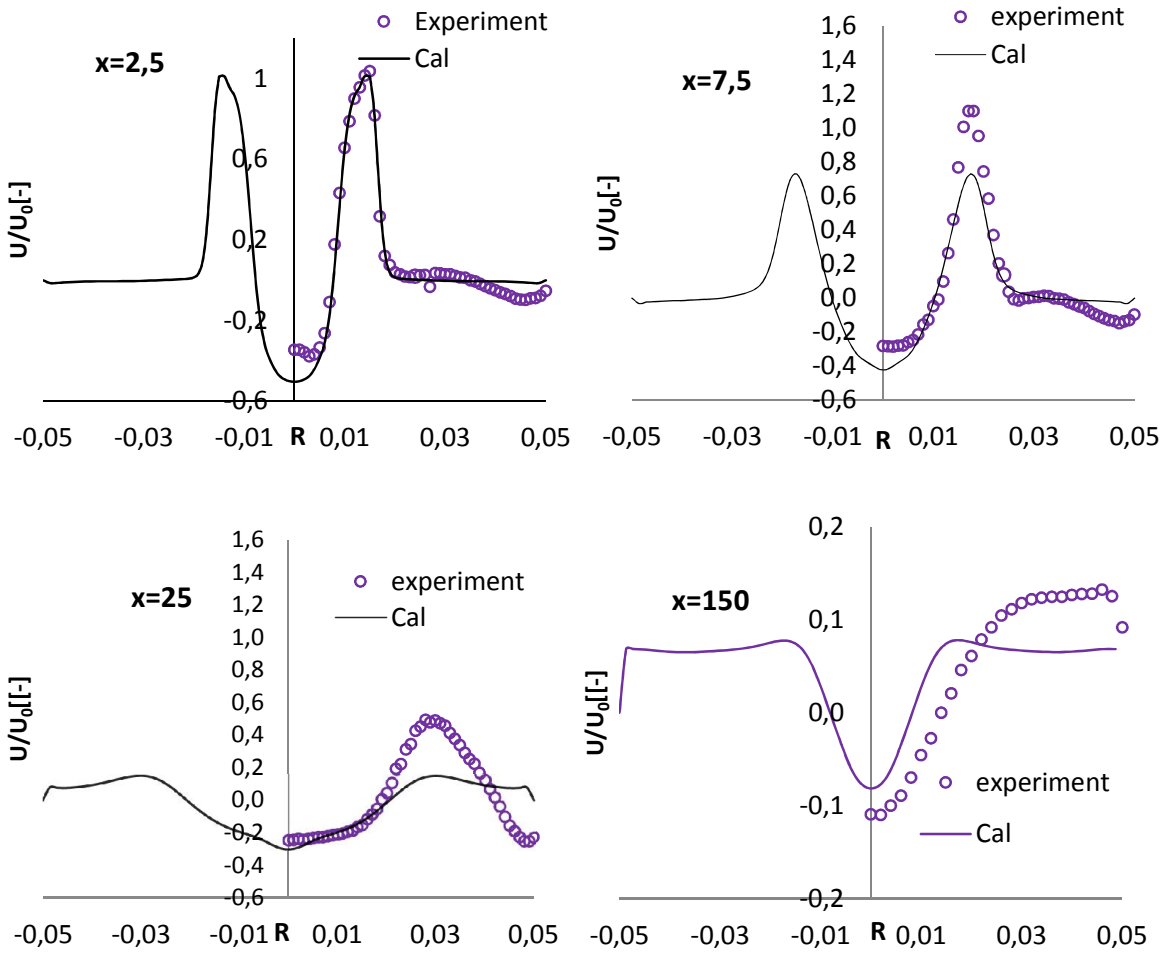

Figure III.4: Axial velocity evolution for different sections

The diagram presents the changes in axial velocity at four different positions along the combustion chamber. At x=2.5, the velocity reaches its peak due to strong swirling and turbulence near the fuel-air injection. As the flow develops downstream at x=7.5 and x=25the velocity gradually decreases, and the profile becomes more symmetric. By x=150, the flow is nearly steady with minimal axial velocity, indicating a fully developed regime. Experimental data shows reasonable agreement with the numerical results, capturing the overall decay and redistribution of momentum along the axis.

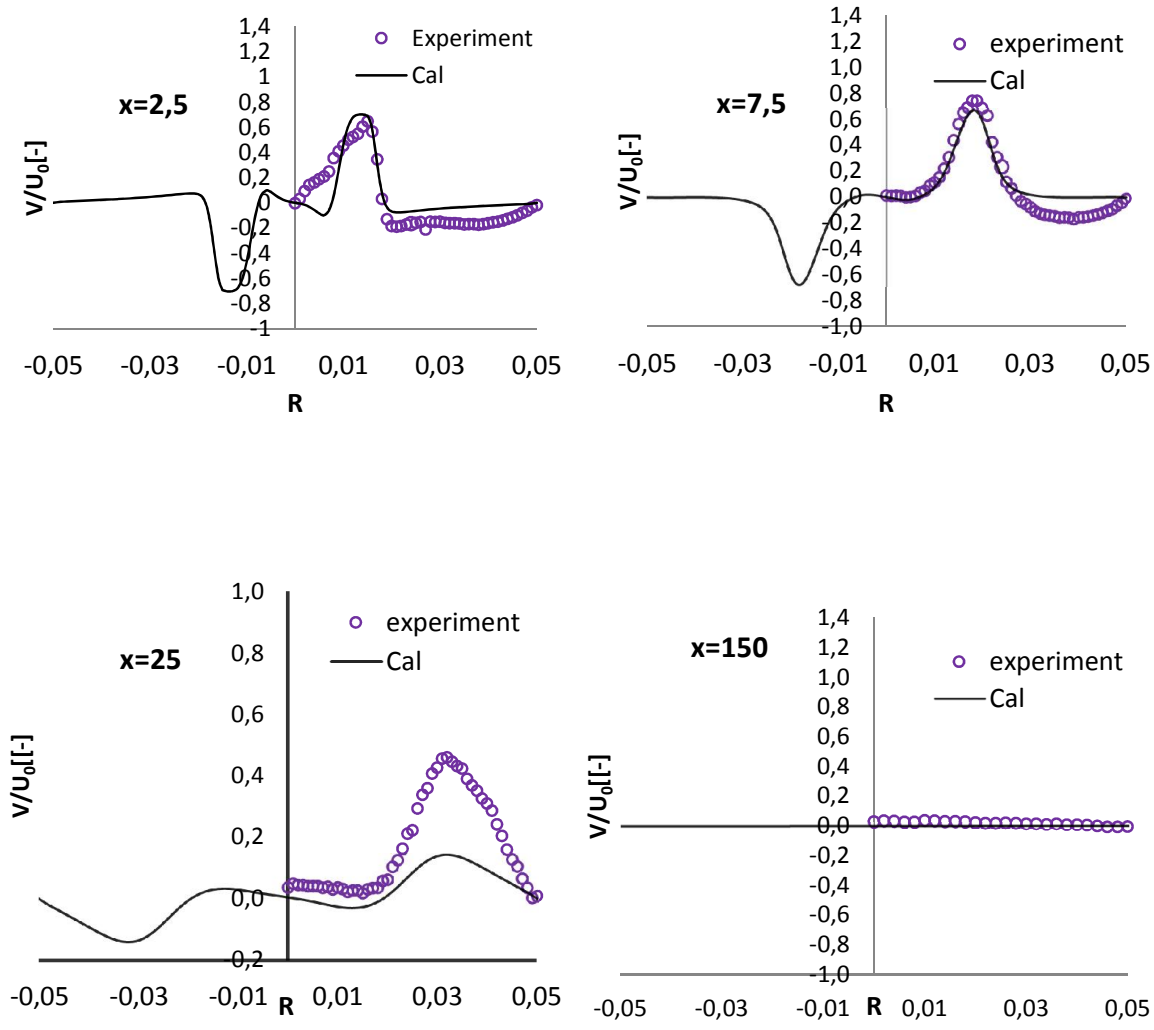

Figure III.5: Radial velocity evolution for different sections

Figure 05 shows the variation of radial velocity at four axial positions in the combustion chamber. At x=2.5, the velocity exhibits strong radial motion due to swirling and flow expansion. As the flow progresses to x=7.5and x=25, the radial component decreases gradually, indicating reduced lateral motion. By x=150, the radial velocity is nearly zero, suggesting a fully aligned axial flow. Numerical results align well with the experimental data, showing a consistent decay in radial momentum.

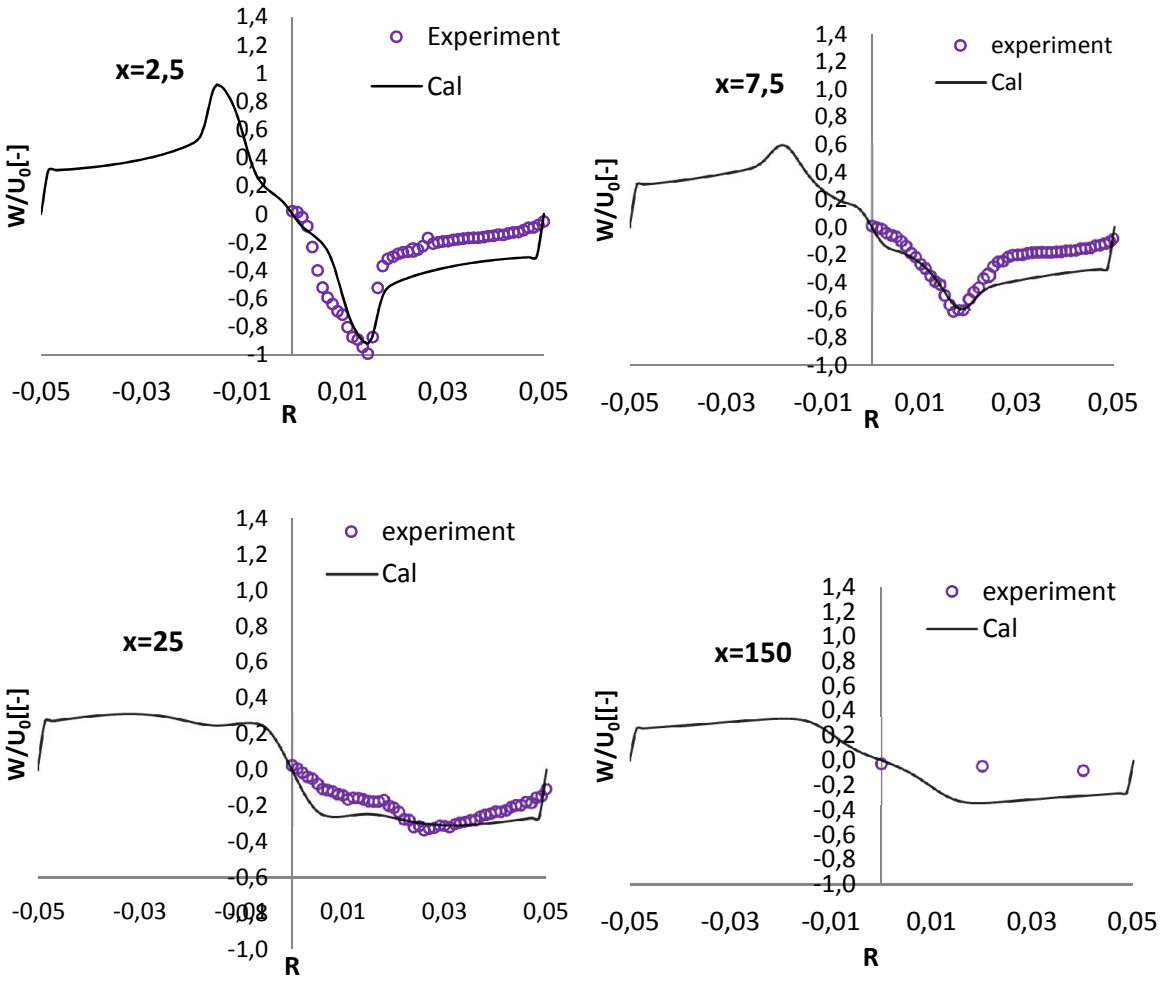

Figure III.6: Tangential velocity evolution for different sections

The variation of tangential velocity has been illustrate in figure 06. Along different axial sections. At x=2.5x , the tangential velocity is pronounced due to the swirl introduced at the inlet. As the flow evolves downstream to x=7.5x and x=25, the tangential component steadily declines. By x=150, the tangential motion is almost fully dissipated, reflecting the transition to an axially dominated flow. The numerical predictions show good agreement with experimental measurements, especially in capturing the swirl decay trend.

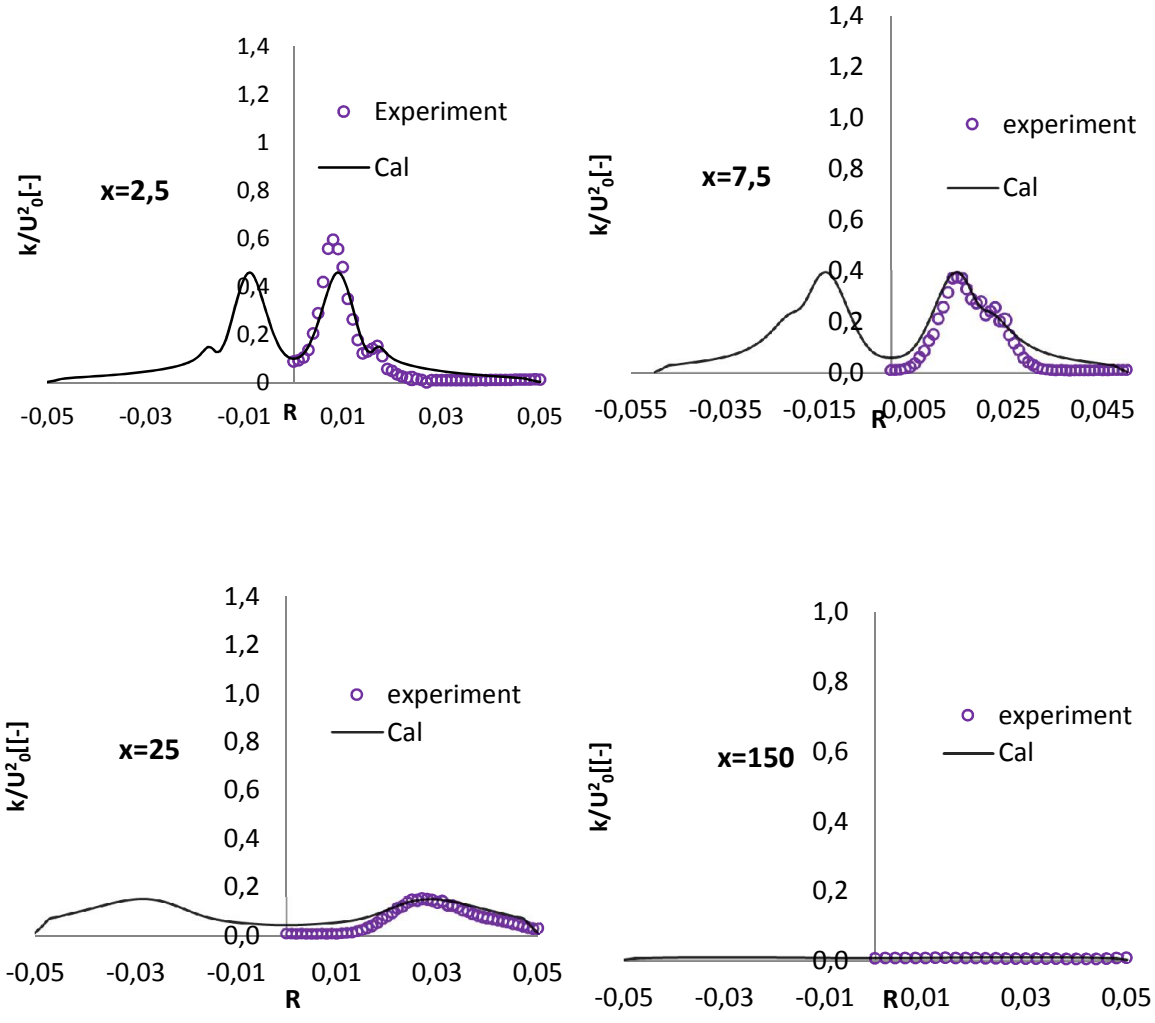

Figure III.7: Kinetic energy evolution for different sections

The figure depicts the distribution of kinetic energy along the axis of the combustion chamber at four different axial positions. At x=2.5, kinetic energy reaches its maximum due to the presence of strong turbulence and swirling immediately following the injection of fuel and air. Further downstream, at x=7.5and x=25, a noticeable reduction in energy is observed as turbulent intensity weakens and the flow begins to exhibit a more uniform structure. By the time the flow reaches x=150, kinetic energy levels are minimal, suggesting a transition to a fully developed and predominantly laminar regime. The experimental measurements correspond closely with the computational results, confirming the expected trend of turbulence dissipation along the flow path.

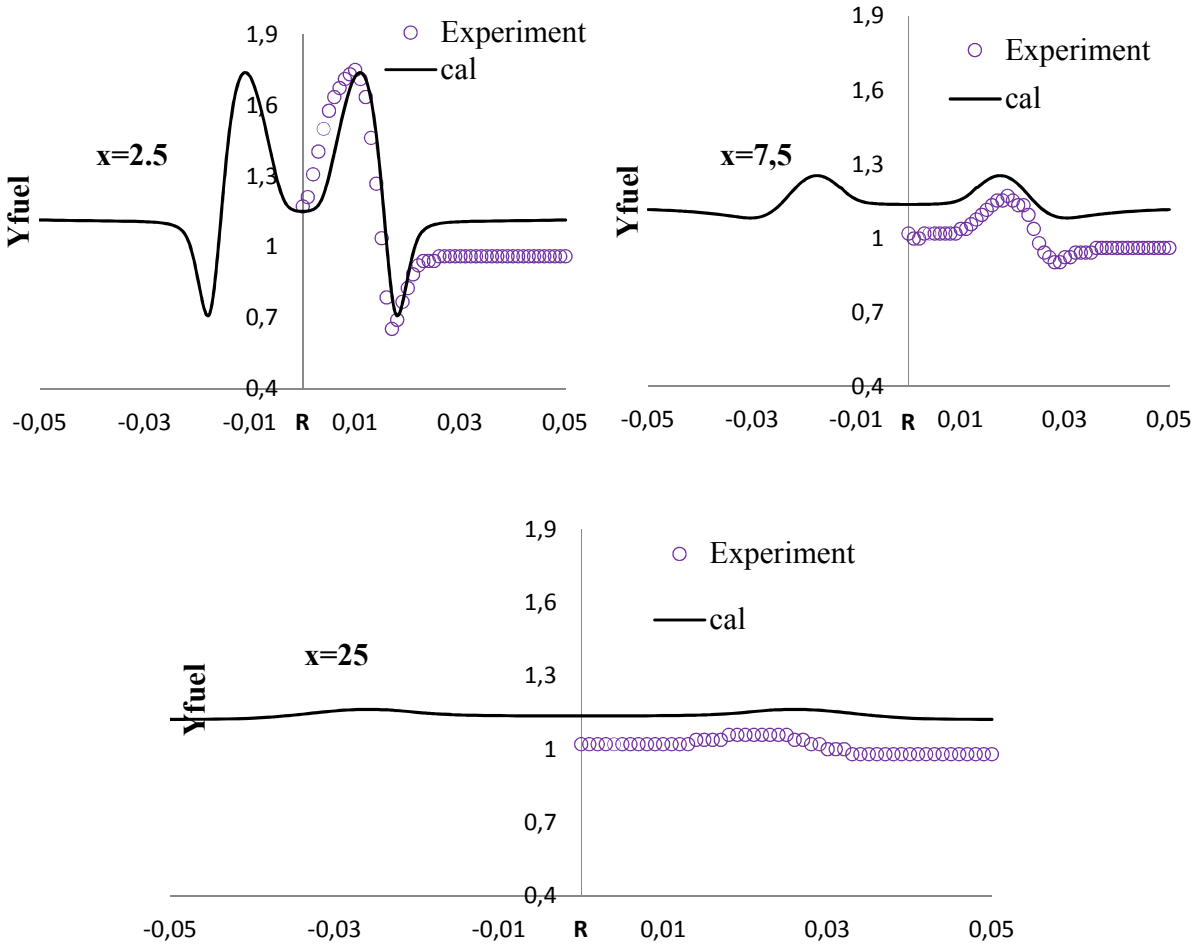

Figure III.8: The fuel mass fraction Y_{Fuel}evolution for different sections.

The figure illustrates the radial distribution of fuel mass fraction Y_{Fuel} at three different axial positions within the combustion chamber for CH□/air non-premixed combustion. At x=2.5, significant fluctuations in the computed profile are observed, indicating the presence of strong turbulence and swirling immediately downstream of the fuel and air injection. The experimental data follow the general trend but exhibit some deviation, likely due to measurement difficulties in this highly turbulent region. Further downstream, at x=7.5, the fluctuations become less pronounced, reflecting a decrease in turbulence intensity and the onset of a more stabilized mixing process. By x=25, the fuel distribution appears nearly uniform, suggesting the transition toward a more developed and less turbulent regime. Across all positions, the computational results show good agreement with the experimental measurements, confirming the predicted trend of turbulence dissipation and progressive stabilization of the flow along the axial direction.

III.5. NOx Formation:

Nitrogen oxides (NOx) are considered major combustion pollutants, primarily including nitric oxide (NO), nitrogen dioxide (NO□), and nitrous oxide (N□O). These pollutants have shown a steady increase in atmospheric concentration since the mid-20th century due to industrial and energy production activities [4,5].

NO is predominantly formed within the flame zone, while NO□ results primarily from post-flame oxidation processes. In contrast, N□O originates mostly from combustion sources under specific operating conditions [4].

There are four primary mechanisms responsible for NO formation during combustion:

III.5.1. Thermal NOx:

Thermal nitrogen oxides are produced via the direct oxidation of molecular nitrogen (N□) at elevated temperatures. This process, commonly referred to as the **Zeldovich mechanism**, involves a set of high-temperature reactions. It is particularly sensitive to temperature, with a rapid increase

in NO formation observed above 1500°C due to the high activation energy required for the reactions to proceed [5].

$$N_2 + O \leftrightarrow NO + N \quad \text{(III.2)}$$

$$N + O_2 \leftrightarrow NO + O \quad \text{(III.3)}$$

$$N + OH \leftrightarrow NO + H \quad \text{(III.4)}$$

The rate-limiting step in NO formation is:

$$N_2 + O \; f \; NO + N \quad \text{(III.5)}$$

Thermal NO formation is highly temperature-dependent, with a significant increase in formation rate at temperatures above 1500°C, due to the high activation energy required (approximately E_a= 319 kJ/mol) [6].

III.5.2. Prompt NOx

Prompt NOx is produced in fuel-rich combustion environments and was first described by Fennimore. It forms in the flame zone because of interactions between atmospheric nitrogen (N□) and hydrocarbon species. The term “Prompt” refers to the early formation of NO near the flame front.

This formation mechanism is influenced by the mixing rate of fuel and air and proceeds through the following reaction steps [5]:

-Reactions between N□ and hydrocarbon fragments produce hydrogen cyanide (HCN):

$$CH + N_2 \leftrightarrow HCN + N \quad \text{(III.6)}$$

-Hydrogen cyanide undergoes hydrogen abstraction reactions with oxy-cyanogen species to form ammonia radicals (NH, NH□):

$$HCN + O \leftrightarrow NCO + H \quad \text{(III.7)}$$

$$NCO + H \leftrightarrow NH + CO \quad \text{(III.8)}$$

-These ammonia radicals further react to form NO:

$$NH + H \leftrightarrow N + H_2 \quad \text{(III.9)}$$

$$N + OH \leftrightarrow NO + H \quad \text{(III.10)}$$

III.5.3. Fuel NOx

Fuel NOx originates from the combustion of fuels containing chemically bound nitrogen, such as certain solid and liquid fuels. This type of NOx is formed when the nitrogen in the fuel is oxidized by excess oxygen during combustion.

As combustion proceeds, nitrogen bound in the fuel is released as free radicals, which may eventually form either NO or N□. The formation of Fuel NOx depends on the stoichiometric ratio between air and fuel. Fuel-rich mixtures typically result in high NOx formation, indicating that this process is largely independent of the fuel type [7].

III.6. Results and discussions:

This curve represents the distribution of static temperature at a fixed distance of 25mm from a reference point under different methane ratios.

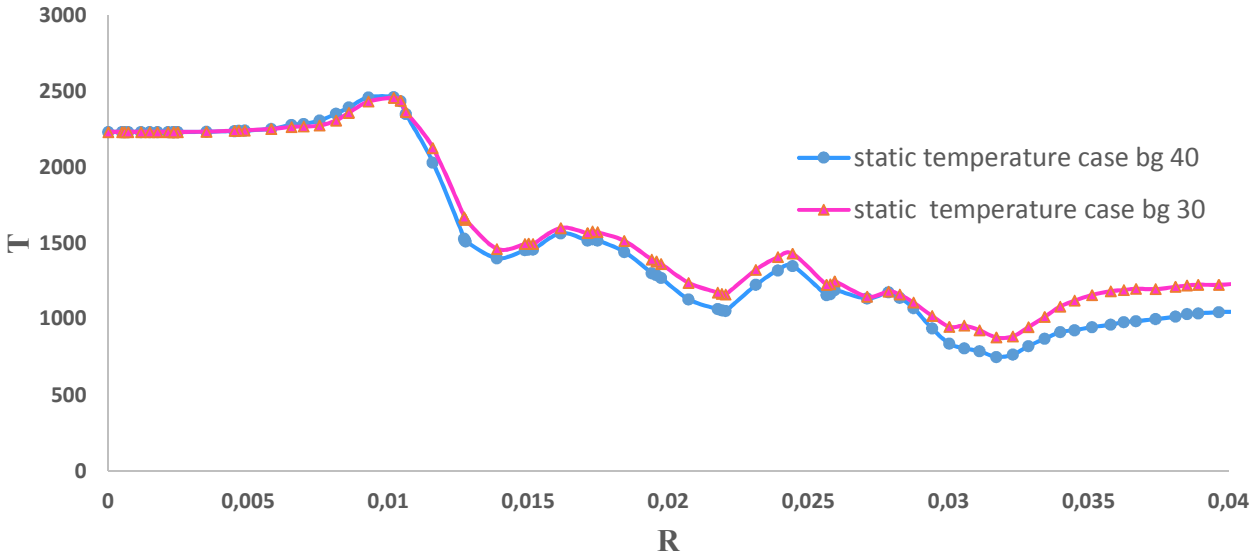

Figure (III.9): static temperature evolution for 40% and 30% hydrogen cases.

The curve represents the distribution of static temperature at a fixed distance of 25 mm from a reference point under different methane ratios. The results show a sharp rise in temperature reaching a peak, followed by a gradual decrease accompanied by fluctuations. When comparing the two cases, it is observed that the case with the lower hydrogen ratio (30%) exhibits higher and more stable temperatures after the peak, whereas the higher hydrogen ratio case (40%) shows a greater drop in temperature with more pronounced fluctuations.

These findings indicate that reducing the hydrogen ratio leads to more efficient combustion and greater thermal stability in the studied region, highlighting the significant influence of fuel composition on flame behavior and thermal characteristics.

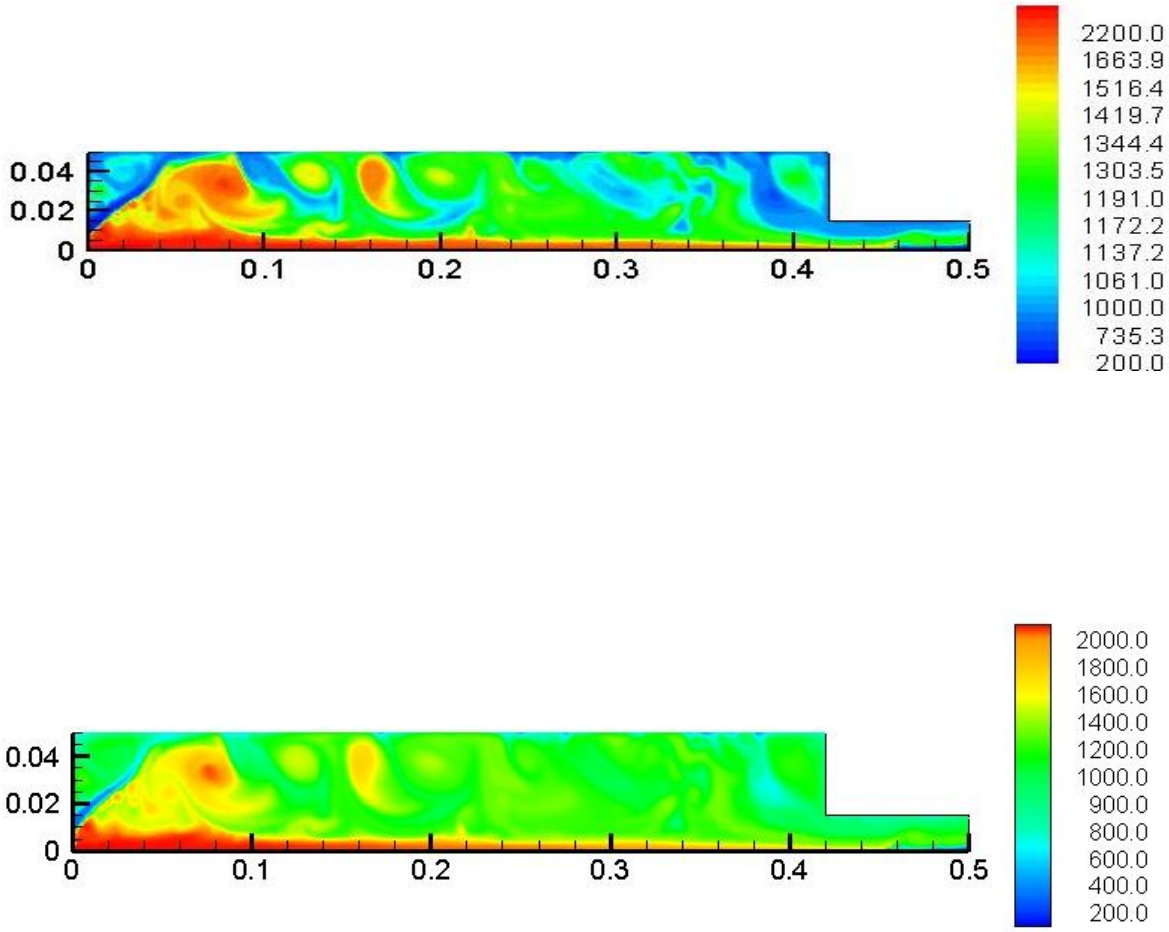

Figure III.10: Description of the heat in the combustion chamber

This curve represents the mass fraction distribution of methane gas (CH□) at a fixed distance (25 mm) from a reference point, under different hydrogen ratios.

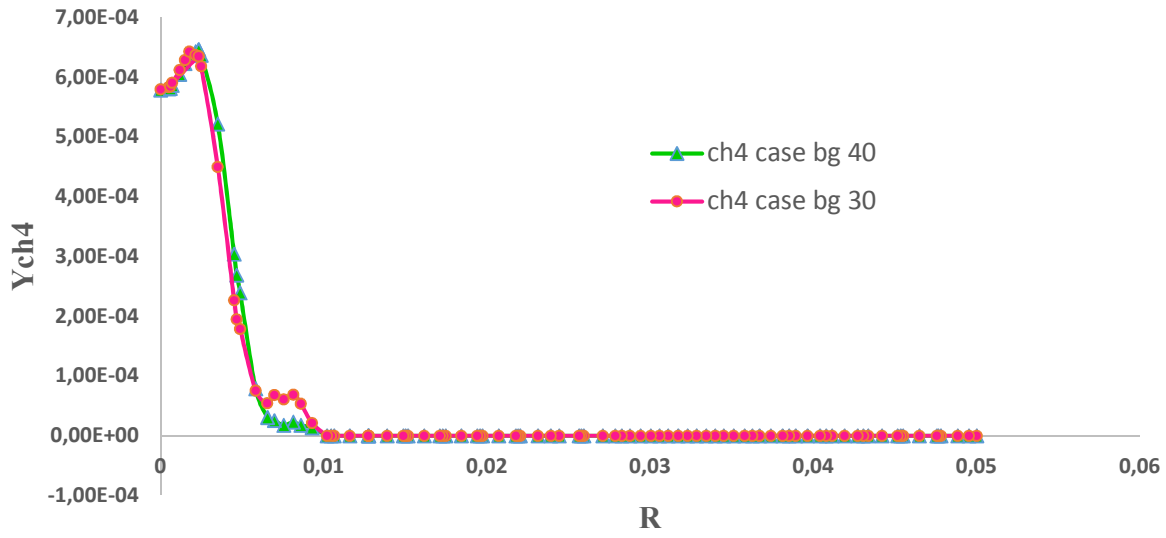

Figure III.11: Mass fraction evolution of CH□ for 40% and 30% hydrogen cases

The curve illustrates the mass fraction distribution of methane (CH□) at a fixed distance of 25 mm from a reference point under different methane ratios. The mass fraction starts at a relatively high value and decreases sharply to near zero levels. The profiles for both cases are very similar, with the case 40 curve beginning at a slightly higher initial value before dropping.

This behavior indicates that methane is rapidly consumed in the early region, suggesting efficient combustion. Although the initial methane content is higher in the 40 case, it is consumed at nearly the same rate as in the 30 case. This suggests that the consumption rate is not significantly affected by the initial methane concentration within the studied range.

This curve represents the mass fraction of carbon dioxide (CO□) at a fixed distance (25 mm) from a reference point, under different hydrogen ratios.

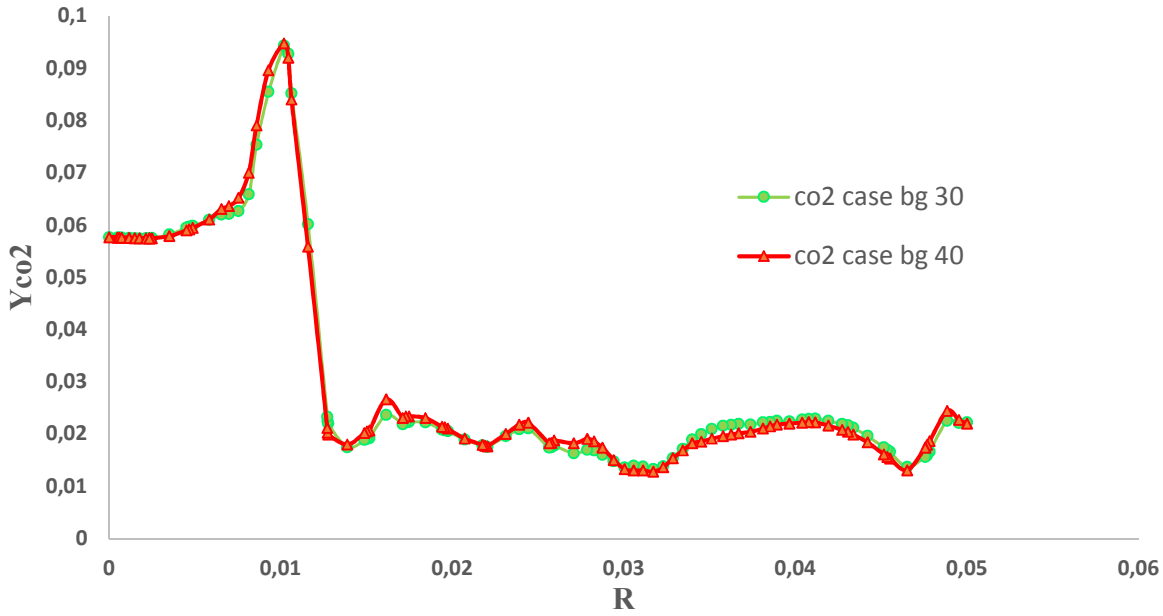

Figure III.12: Mass fraction evolution of CO_2 in 40% and 30%cases

The curve shows the mass fraction distribution of carbon dioxide (CO□) at a fixed distance of 25 mm from a reference point under different hydrogen ratios. A gradual increase is observed at the beginning, reaching a clear peak around 0.01 m, followed by a sharp drop and mild fluctuations. The profiles for both cases are nearly identical, with very close values throughout the domain.

This indicates that CO□ is produced efficiently and reaches its maximum concentration quickly, reflecting active combustion in a localized region. The similarity between the two cases suggests that the methane ratio does not significantly influence the amount of CO□ produced at the studied location. The post-peak fluctuations may be attributed to gas mixing or the slowing down of the reaction.

- This curve represents the mass fraction distribution of carbon monoxide (CO) at a fixed distance (25 mm) from a reference point, under different hydrogen ratios.

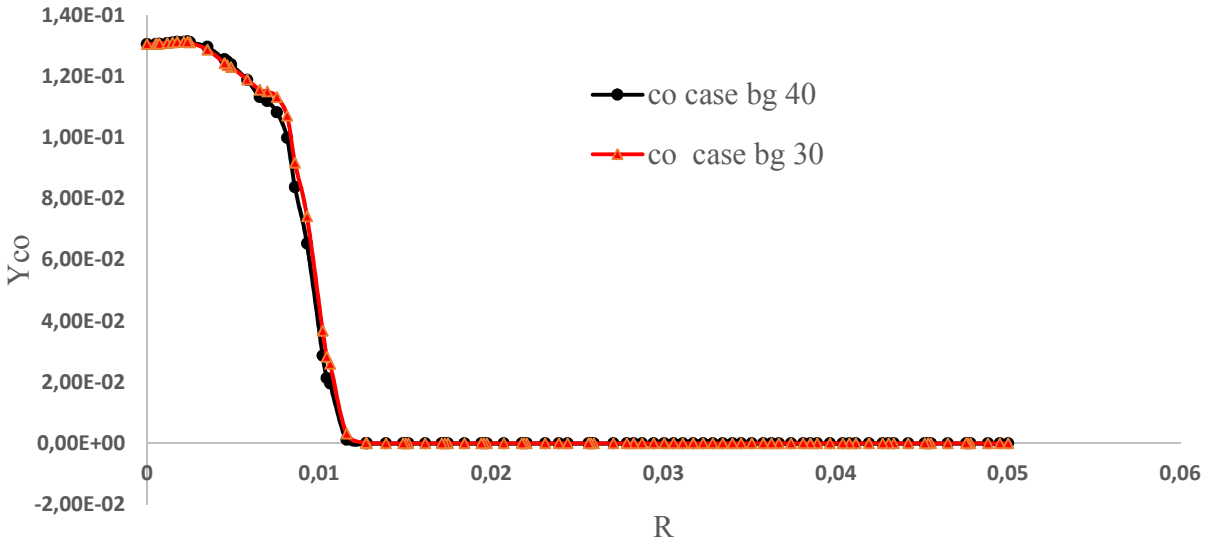

Figure III.13: mass fraction of CO evolution for 40% and 30% hydrogen cases

As depicted in the figure, the curve represents the mass fraction distribution of carbon monoxide (CO) measured at a fixed axial position 25 mm downstream from the reference point, under two different hydrogen concentrations (40% and 30%). Initially, the CO mass fraction exhibits elevated values forming a distinct plateau, followed by a sharp decline around the axial location of 0.01 m. Beyond this point, the CO levels stabilize near zero with minimal fluctuations. Both cases display nearly identical trends, suggesting that CO formation and consumption dynamics are largely unaffected by the change in methane concentration at this specific location. The abrupt decrease in CO indicates the presence of a localized combustion region where CO is rapidly oxidized, likely to CO□.

The minimal difference between the two cases implies that the methane ratio does not significantly influence the CO distribution at this distance. The slight post-drop fluctuations may be due to

residual mixing effects or minor chemical reactions still occurring beyond the main combustion zone.

This curve (figure III.15) represents the mass fraction of Pollutant no at a fixed distance (25 mm) from a reference point, under different hydrogen ratios.

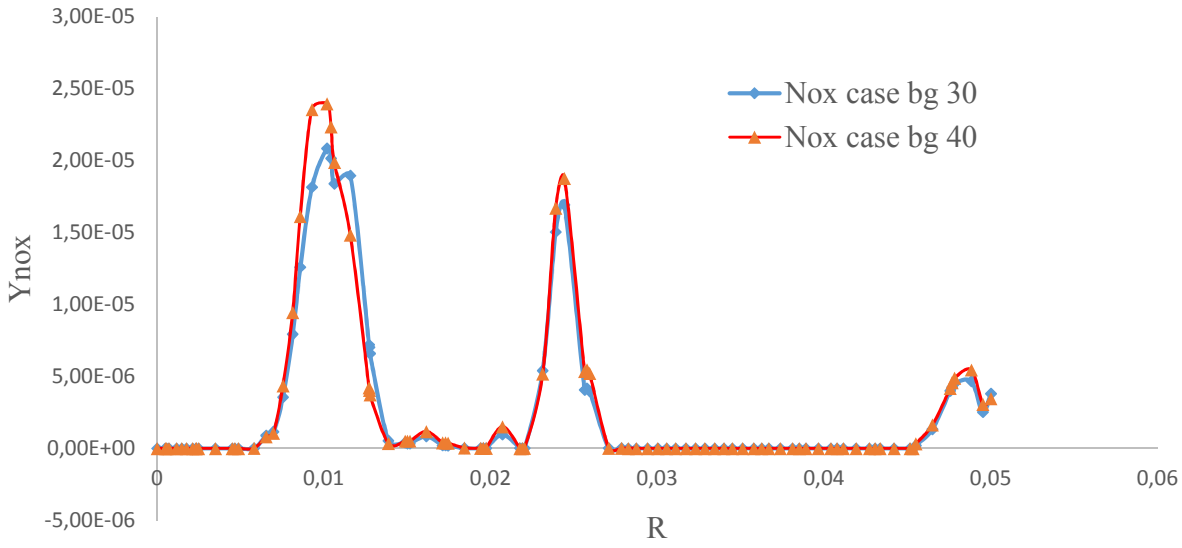

Figure III.14: Mass fraction of Pollutant no in the case of 40% and 30% hydrogen

The figure the mass fraction distribution of nitric oxide (NO) at a fixed distance of 25 mm from a reference point under different hydrogen ratios. Initially, the NO mass fraction is near zero but quickly increases, forming two distinct peaks one around 0.01 m and another near 0.023 m before rapidly declining. After this decline, the NO values remain low with only minor fluctuations for the rest of the domain.

Both profiles (case 40 and 30) follow a similar pattern, but the 40% methane case exhibits slightly higher peak values, particularly around the first maximum. This suggests that a higher hydrogen concentration leads to increase NO formation in the early stages of combustion, likely due to higher flame temperatures and enhanced thermal NO mechanisms. The rapid rise and fall of NO indicate localized high-temperature zones where NO is primarily formed and then diluted or transported

away. The overall similarity between the two cases implies that while the methane ratio influences the peak magnitude, the general formation and reduction behavior of NO remains comparable at this measurement location. The small post-peak variations may result from turbulent mixing or slow residual reactions in the exhaust region.

Reference:

[1]. Furuhata, T., Amano, S., Yotoriyama, K., & Arai, M. (2007). Development of can-type low NOx combustor for micro gas turbine. Fuel, 86(17–18), 2463–2474.

[2]. Lalmi, D., & Hadef, R. (n.d.). Numerical study of the swirl direction effect at the turbulent diffusion flame characteristics. International Journal of Heat and Technology, 35(3), 520–528.

[3]. Merkle, K., Haessler, H., Büchner, H., & Zarzalis, N. (2003). Effect of co- and counter-swirl on the isothermal flow and mixture field of an airblast atomizer nozzle. International Journal of Heat and Fluid Flow, 24(4), 529–537

[4]. Cavaliere, A., & de Joannon, M. (2020). NO is predominantly formed within the flame zone, while NO□ results primarily from post-flame oxidation processes. In contrast, N□O originates mostly from combustion sources under specific operating conditions.

[5]. United States Environmental Protection Agency (EPA). (1999). Nitrogen oxides (NOx): Why and how they are controlled. Office of Air Quality Planning and Standards.

[6]. Claypole, T. C., & Syred, N. (1981). The effect of swirl burner aerodynamics on NOx formation. Proceedings of the Combustion Institute, 18, 81–89.

[7]. ANSYS Inc. (2013). ANSYS Fluent theory guide (Release 15.0). ANSYS Inc.

General conclusion

After this academic work, which was dedicated to the assessment of biogas combustion in a turbulent diffusion flame, it can be said that the study has helped shed light on the importance of using renewable energy sources, particularly biogas, as a promising and sustainable alternative to conventional energy sources. Through theoretical analysis and numerical simulation, a deeper understanding was achieved regarding flame behavior under the influence of various factors, such as the blending ratio of methane and hydrogen, and the flow conditions within the combustion chamber.

The results showed that improving the performance of biogas combustion requires not only knowledge of the fuel composition but also control over the dynamic and thermal conditions that affect its stability and efficiency. Numerical simulation tools enabled a precise study of flame behavior, thermal distribution, and emissions, which would be difficult to achieve through experimentation alone. This highlights the importance of such tools in scientific research and modern engineering.

On the other hand, this study does not represent the end of research in this field, but rather opens avenues for more specialized future studies. These could investigate the effects of additional variables, such as operating pressure, burner design, or the use of various types of biofuels. The work can also be expanded toward the experimental side to support and validate the obtained results in real-life conditions.

Finally, we hope that this thesis, with its scientific data and detailed analyses, contributes to enriching the knowledge in the field of renewable energies and gas combustion, and serves as a useful reference for students, researchers, and engineers interested in developing efficient and clean energy solutions that support sustainable development.

République Algérienne Démocratique et Populaire
وزارة التعليم العالي والبحث العلمي
Ministère de l'Enseignement Supérieur Et de La Recherche Scientifique

Faculté des Sciences et Technologies
جامعة غرداية
كلية العلوم والتكنولوجيا

Département des Enseignements Communs en Sciences et de la Technologie
قسم التعليم المشترك في العلوم والتكنولوجيا

Université de Ghardaïa

غرداية في : ..2..0..جويلية..2025..

إذن بالطباعة (مذكرة ماستر)

بعد الاطلاع على التصحيحات المطلوبة على محتوى المذكرة المنجزة من طرف الطلبة التالية أسماؤهم:

1. الطالب (ة) : (بن احمد زينب) BENAHMED Zineb
2. الطالب (ة) : (لعور فريال) LAOUAR Ferial

تخصص: فيزياء طاقوية وطاقات متجددة

نمنح نحن الأستاذ (ة):

الاسم واللقب	الرتبة – الجامعة الأصلية	الصفة	الامضاء
سبع الحاج يحي	MCA_Univ Ghardaia	الرئيس	
بن شادي وسيلة	MCB_Univ Ghardaia	مصحح (1)	
لغويطر أم كلثوم	MCB_Univ Ghardaia	مصحح (2)	
العلمي الجموعي	Professeur _Univ Ghardaia	مؤطر	

الإذن بطباعة النسخة النهائية لمذكرة ماستر الموسومة بعنوان

....Assessment of the combustion of biogas in a turbulent diffusion flame.....

امضاء رئيس القسم

رئيس قسم التعليم المشترك في العلوم والتكنولوجيا
شويحة فيصل

جامعة غرداية ★ قسم التعليم المشترك في العلوم والتكنولوجيا ★ كلية العلوم و التكنولوجيا